and G3364A) were found in FH1. Anti-factor H antibody was not detected.

Patient 3 (B-12). We analyzed for factor H status using patient's serum, obtained after 7-yrs from the first episode. Factor H level was significantly increased (131% of healthy volunteer's serum, $p < 0.01$). The heterozygous G3717A mutation and two heterozygous disease risk polymorphisms (C994A and G1492A) were found in FH1. In addition, we found the novel silent mutation [C3013T (His980His)] in exon 18. Anti-factor H antibody was not detected.

Patient 4 (C-6). We analyzed for factor H status using patient's serum, obtained after 2-months from the first episode. Factor H level was significantly decreased (74% of healthy volunteer's serum, $p < 0.01$); however, we found neither mutation nor disease risk polymorphism of aHUS in FH1. Anti-factor H antibody was not detected.

Patient 5 (D-3). We analyzed for factor H status using patient's serum, obtained after 4-yrs from the episode. Factor H level was significantly decreased (64% of healthy volunteer's serum, $p < 0.01$); however, we confirmed that this patient had neither mutation nor disease risk polymorphism of aHUS in FH1. Anti-factor H antibody was not detected.

Patient 6. We analyzed for factor H status using patient's serum, obtained after 6-months from the episode. Serum factor H level was significantly decreased (62% of healthy volunteer's serum, $p < 0.01$). We found neither mutation nor disease risk polymorphism of aHUS in FH1, however, we could detect anti-factor H antibody.

Patient 7. We analyzed for factor H status using patient's serum, obtained on admission. Although serum factor H level was normal, we found heterozygous polymorphisms of A C-257T, C994A, and G3364A in FH1. Conservative therapy slowly improved his clinical condition and increased serum factor H level (138% of healthy volunteer's serum, $p < 0.01$). Anti-factor H antibody was not detected.

Patient 8. We analyzed for factor H status using patient's serum, obtained on admission. Serum factor H level was significantly increased (145% of healthy volunteer's serum, $p < 0.01$). The homozygous polymorphisms of C-257T, A2089G, G2881T, and the heterozygous G1492A polymorphism were found in FH1. Furthermore, we found C3645T (Ser1191Leu) mutation in exon 23 (data not shown). Anti-factor H antibody was not detected.

Patient 9. We analyzed for factor H status using patient's serum, obtained on admission. Serum factor H level was significantly increased (125% of healthy volunteer's serum, $p < 0.01$). The homozygous polymorphisms of C-257T, A2089G, G2881T were found in FH1. Anti-factor H antibody was not detected.

Patient 10. We analyzed for factor H status using patient's serum, obtained on admission. Serum factor H level was also significantly decreased (80% of healthy volunteer's serum, $p < 0.01$). We found the homozygous polymorphisms of C-257T, A2089G, G2881T were found in FH1, and detected anti-factor H antibody.

3.2. Pedigree analysis

Further, to clarify the impact of factor H genetic status on the development of aHUS, we analyzed *FH1* mutations and polymorphisms in family members of above 5 patients, and investigated their clinical histories.

3.2.1. Family A

The pedigree of family A is shown in Fig. 1A. We identified that a G3717A mutation of the proband [A-6 (Patient 1)] was inherited from a paternal allele (A-4), and that all three polymorphisms (C-257T, A2089G, G1492A) was from a maternal allele (A-5). The allele sequences of the paternal grandfather (A-1), who died of thrombocytopenic purpura (TTP), were able to be determined from those of the paternal grandmother (A-2) and a paternal uncle (A-3). Taken together, a G3717A mutation of the proband was proved to have originated from paternal grandfather.

3.2.2. Family B

The pedigree of family B is shown in Fig. 1B. Two probands [B-11 (Patient 2) and B-12 (Patient 3)] are cousins to each other, and their maternal grandfather (B-1) had died of juvenile renal insufficiency at age 42 yrs. We identified a G3717A mutation in both probands (B-11 and B-12) that was inherited from each mother (B-9 and B-10), respectively, by taking into consideration of pedigree analysis results and their clinical histories, and estimated that the mutation containing the allele originated from B-1. Further, we estimated that the three polymorphisms (C-257T, A2089G, and G2881T) of their mother's eldest sister (B-3), who has intermittent episodes of recurrent renal insufficiency, were inherited from the other allele of B-1. The *FH1* in B-5 was not able to be determined. B-4, B-6, B-7, and B-8 had already died of other causes.

3.2.3. Family C

The pedigree of family C is shown in Fig. 1C. Similar to the proband [C-6 (Patient 4)], her elder brother (C-4, 33-yr-old) and nephew (C-8, 7-yr-old) had been diagnosed as aHUS. However, their *FH1* were not able to be analyzed in present study. Her mother (C-2) had three heterozygous polymorphisms (C-257T, A2089G, and G2881T), but had no episodes of HUS. Her elder sister (C-3) inherited these three polymorphisms without episodes of HUS; whereas, the proband (C-6) did not inherit any of those polymorphisms.

3.2.4. Family D

The pedigree of family D is shown in Fig. 1D. The proband's mother (D-2) without episodes of HUS had three heterozygous polymorphisms (C-257T, A2089G, and G2881T). The proband [D-3 (Patient 5)] did not inherit any polymorphisms from her mother.

3.3. Biochemical characterization of factor H in aHUS patients

To characterize factor H in aHUS patients' sera biochemically, we performed immunoblot analysis using specific antibody against factor H. We detected the main band with a molecular weight of 150 kDa, corresponding to factor H protein, and the faint band with a molecular weight of 43 kDa, corresponding to factor H-like-protein 1 (Zipfel & Skerka, 1999; Ault, 2000), in all subjects. As well as in normal control, no extra band was observed in all subjects (data not shown).

Further, to investigate the function of factor H, we carried out the hemolytic assay using sheep erythrocytes as described in Section 2. The reference value of the percent hemolytic activity was determined by making measurements of 32 healthy volunteers' sera. The individual differences in the percent hemolytic activities were minimum at 5% serum concentration among serum dilution series (CV, 14%); thus, we defined the mean hemolytic activity at 5% serum concentration as a provisional reference value (mean $\pm$ 2SD, $12 \pm 3\%$). We then compared the percent hemolytic activity of each patient's serum with the reference value. Five of 10 aHUS patients (Patients 1, 3, 6, 7, and 8) presented with a significantly high level of hemolytic activity (Fig. 2). When we added recombinant factor H, with a final concentration of 1.1 mg/dl, significantly suppressed the accelerated hemolytic activities of 5 all patients (data not shown). Three of these 5 patients (Patients 1, 3, and 8) had mutation in exon 23 that encodes for SCR 20. Patient 4 had neither mutation nor polymorphism, despite having a low level of serum factor H. Patient 5 had three heterozygous polymorphisms, but no mutations, with a normal level of serum factor H. On the other hand, although Patient 2 had a mutation in exon 23, his hemolytic activity exhibited the normal level. Overall, no correlation between the hemolytic activity

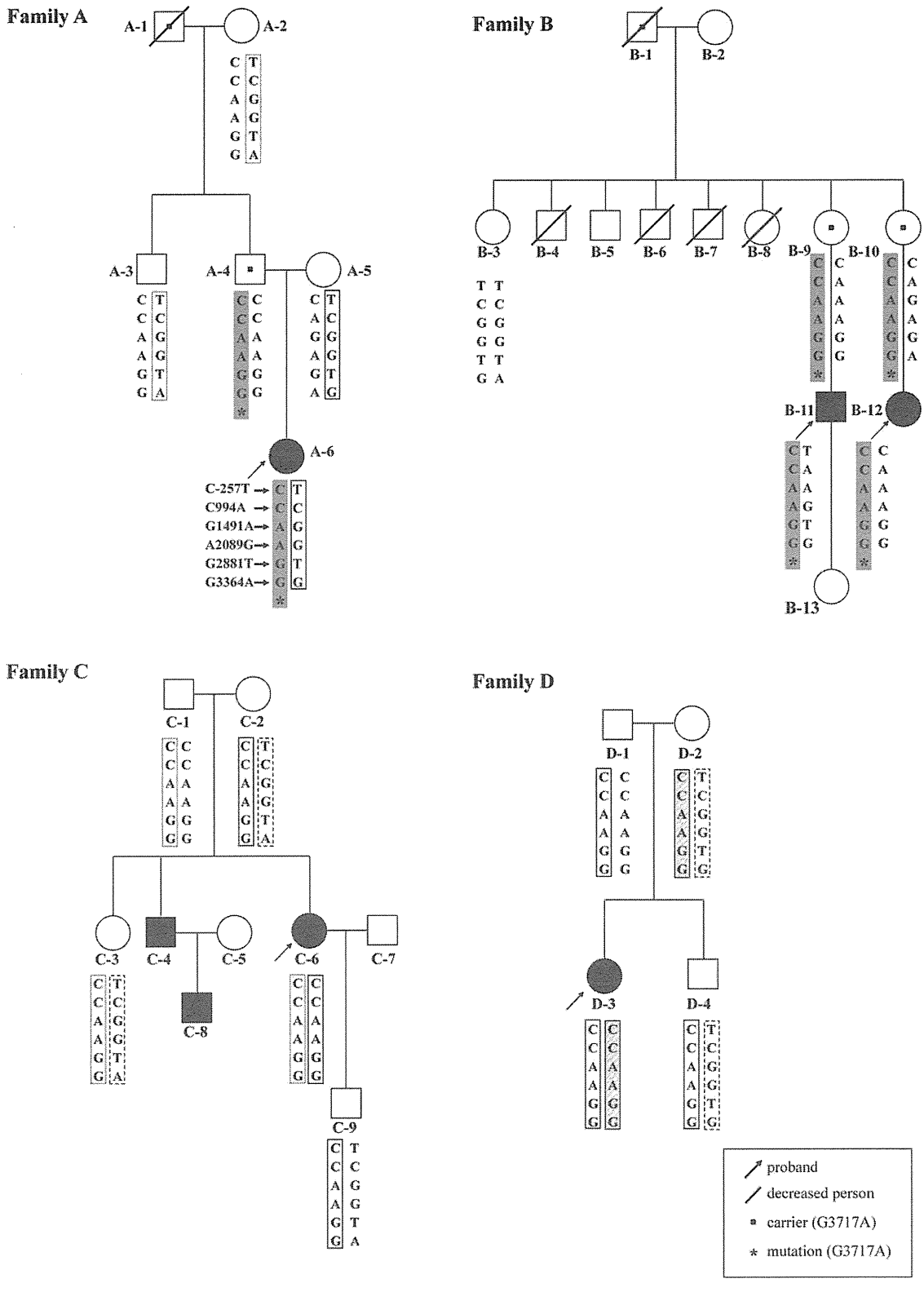

Fig. 1. Pedigree of families A, B, C, and D. We analyzed the data for mutations and polymorphisms in *FH1* as described in Section 2. Arrows, probands; squares, men; circles, women; slashes, deceased; black asterisk, G3717A mutation; central black squares, carriers of G3717A mutation.

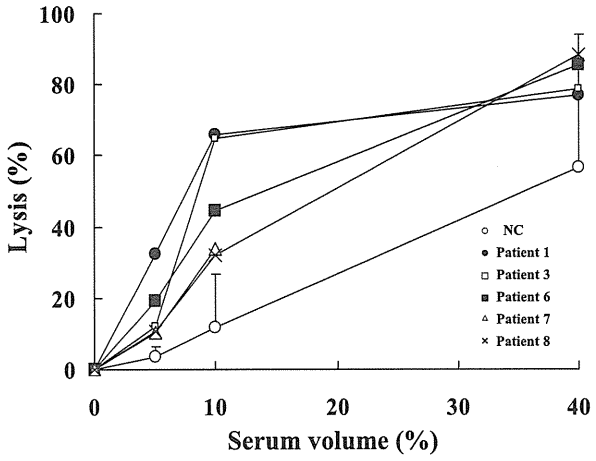

Fig. 2. Hemolytic assay. Lysis of sheep erythrocytes by serum obtained from aHUS patients [solid circles, Patient 1 (with G3717A); open square, Patient 3 (with G3717A), solid square, Patient 6 (without mutation); triangles, Patient 7 (without mutation); crosses, Patient 8 (with C3645T mutation)]. The percent hemolytic activity of 32 healthy volunteers' sera shown (open circles) are mean + 2SD. (b) Inhibition of the lysis by factor H. We added recombinant factor H to each patients' serum to give final factor H concentrations of 1.1 mg/dl. Lysis (%) [with (shaded bars) or without (open bars) recombinant factor H] was determined at 5% serum concentration after a 30-min incubation. Data are expressed as mean ± 2SD from duplicate determinations in each of three separate experiments. *: $P < 0.05$ and **: $P < 0.01$ compared with the lysis (%) of each patient serum without recombinant factor H.

and factor H level was observed. The specificity of a hemolytic assay for the detection of aHUS was insufficient (50%), but the sensitivity was 100%.

3.4. Allele frequencies of factor H gene mutations and polymorphisms

To evaluate the effects of mutations and polymorphisms in *FH1* on the development of aHUS in Japanese, we compared the frequency of *FH1* mutations and polymorphisms in aHUS patients with that in healthy volunteers. As summarized in Table 3, no significant differences in the frequencies of all 6 disease risk polymorphisms, identified previously (Caprioli et al., 2003), were observed between aHUS patients and healthy volunteers. However, the mutations in exon 23 of FH1 (A3717G or C3645T) were highly frequent, but not statistically significant, detected in aHUS patients (40%).

4. Discussion

In the present study, we identified *FH1* mutation in 4 of 10 aHUS patients. All of those mutations, located in exon 23 of *FH1*, encode SCR 20 (3 Arg1215Gln mutations and 1 Ser1191Leu mutation). Previous studies demonstrated that the majority of the mutations associated with aHUS are clustered at the SCR 20 in C-terminal end of factor H molecule, which plays a critical role as both C3 (C3d fragment)- and heparin-binding sites (Blackmore et al., 1998; Ault, 2000; Caprioli et al., 2001). Three of these patients presented with a significantly high level of hemolytic activity. The serum factor H level of Patient 1 was only modestly decreased, and those of Patient 3 and Patient 8 were increased rather than decreased. These findings supported the notion that those mutations in SCR 20 may impair the function of factor H in the alternative complement cascade on cell surface (Rodríguez de Córdoba et al., 2004) and subsequently cause the development of aHUS.

Hemolytic assays using sheep erythrocytes have been thought to be useful for the detection of factor H-related complement regulatory defects and molecular diagnosis of factor H-related aHUS (Sánchez-Corral et al., 2004). Notably, however, we revealed several discrepancies between the existence of the *FH1* mutation and the results of hemolytic assays in three cases. First, two patients (Patient 6 and Patient 7) presented with significantly high levels of hemolytic activity, even though they had no mutations in the well-known hot spot of *FH1*. In case of Patient 6, autoantibody may possibly interfere with the reaction on the quantification of serum factor H as described previously (Dragon-Durey et al., 2005; Józsi et al., 2007). It differed from Patient 6 with a low level of serum factor H, interestingly, Patient 7 presented with a normal level of serum factor H. Although we could not exclude the influence of some medical treatments (especially, plasma infusion) on specimens, used for the quantification of serum factor H, the addition of recombinant factor H markedly improved hemolytic activities of both patients, providing compelling evidence that these patients have factor H-related complement regulatory defects, attributed to some variants in other region of *FH1*, which were not analyzed in present study. In general, mutations are categorized into the type I mutations with a significant reduction of the coded proteins and the type II mutations with an anomalous activity of the coded proteins. Our findings suggested that Patient 7 possibly carry some type II mutations. Second, despite the presence of Arg1215Gln mutation in SCR 20, one patient (Patient 2) presented with a normal or slightly high level of hemolytic activity. While the reduction of serum C3 in this patient arguably indicated that a complementary pathway was excessively activated, serum factor H level in this patient was slightly increased; thus, one possible reason for this discrepancy is that the dysfunction of innate factor H may cause up-regulation of factor H production, even an immature one. Further studies will be necessary to clarify the reason for these discrepancies.

We showed that 4 of 10 aHUS patients presented with normal levels of hemolytic activity and without any mutations in SCR 20. We could detect anti-factor H antibody in serum of Patient 10; therefore, autoantibody may possibly interfere with the reaction on the quantification of serum factor H. Although the pathogenesis of Patient 9 was difficult to interpret only by the results of the present study, those of other 2 patients (Patient 4 and 5) could be supposed to be caused by the reduction of serum factor H level. This finding suggests the possibility that the production of mature factor H protein might be impaired by some *FH1* abnormality, such as aberrations in alternative splicing, based on the mutation in the region of *FH1* introns. Atkinson et al. (2005) previously demonstrated that approximately 50% of patients with aHUS have a mutation in one of three genes, encoding factor H (20–30%), MCP (10–20%), or factor I (10–20%). Hence, we also should take account of the aberrations in other complementary regulatory factors, and so it will be necessary to do additional experiments.

The results of pedigree analysis for family A and B also supported the notion that a mutation in the region of *FH1*, encoding SCR 20 of factor H, could be one of potent causative risk factors for the development of aHUS, although the proband's father (A-4) in family A and both probands' mother (B-9 and B-10) in family B had no episodes, even though they had this mutation. In contrast, we could not find any remarkable features in *FH1* in the pedigree analysis for family C and D. However, as described above, we cannot completely deny the factor H dysfunction, derived from some aberration of *FH1*. The marked reduction of serum factor H level in Patient 4 (C-6) leads to the above conclusions. In particular, despite having no episodes, her son (C-9) also presented with marked reduction of serum factor H level, suggesting that he might inherit some aberration of *FH1* (possibly some type I mutations in *FH1*) from his mother [Patient 4 (C-6)], but not any effects of autoantibodies. Furthermore, the clinical differences between Patient 4 (C-6) and her son (C-9) suggested that aberrations of *FH1* may not be an independent risk factor for aHUS. As described previously (Rodríguez de Córdoba et al., 2004; Noris & Remuzzi, 2009), other triggers may promote the development of aHUS. In fact, Patient 4 (C-6) had relapsed after pregnancy

and partum. She also presented with an upper respiratory tract inflammation at relapse. These clinical findings were of importance to clarify the detailed pathogenic mechanism of aHUS.

Caprioli et al. (2003) and Neumann et al. (2003) previously reported that several polymorphisms in *FH1*, so-called disease risk polymorphisms, are frequently detected in aHUS patients more than healthy volunteers in Caucasians and German registries, respectively. We examined the allele frequencies of those disease risk polymorphisms in Japanese populations (see Section 2). Of interest, no significant difference in frequency of disease risk polymorphisms was observed between healthy volunteers and aHUS patients in Japanese groups, although the present study includes a limitation in that the results were obtained from small mass analyses. Previous studies (Blom et al., 2008; Martínez-Barricarte et al., 2008) have demonstrated racial differences in the relevance of a polymorphism in the C4b-binding protein, a regulator of the classical pathway of complementary activation, in the development of aHUS. Similarly, our findings suggest that ethnicity may affect the linkage between carrying the disease risk polymorphism in factor H and the development of aHUS.

In conclusion, our results are consistent with those of prior studies for other populations showing that FH1 mutations relates to the development of Japanese aHUS; whereas, of interest, the well-known disease risk polymorphisms of FH1 have been detected in most healthy Japanese. This finding suggested that some 'second hit' (e.g., a mutation in FH1, unknown polymorphisms in FH1, or variants of other complement regulatory factors) may be required for factor H polymorphism to be a risk factor of Japanese aHUS.

Competing interests

None.

Ethical approval

The study was approved by the ethics committee of Shinsyu University (approval No., 221).

Guarantor

KY.

Contributorship

KY has designed and supervised the project, SM, YH, MH, and KM have carried out the project, SM has written the first draft of the manuscript, NF, YK and SK have been the laboratory methods consultants, and KK and TH commented on drafts of the manuscript.

Acknowledgements

We gratefully acknowledge Dr Toshiko Kumagai and Dr Mitsutoshi Sugano (Department of Laboratory Medicine, Shinshu University Hospital) for their advices and encouragement. This work was partially supported by Nagano Society for the Promotion of Science.

References

Atkinson, J.P., Liszewski, M.K., Richards, A., Kavanagh, D., Moulton, E.A., 2005. Hemolytic uremic syndrome: an example of insufficient complement regulation on self-tissue. Ann. N. Y. Acad. Sci. 1056, 144–152.

Ault, B.H., 2000. Factor H and the pathogenesis of renal diseases. Pediatr. Nephrol. 14, 1045–1053.

Blackmore, T.K., Hellwage, J., Sadlon, T.A., Higgs, N., Zipfel, P.F., Ward, H.M., Gordon, D.L., 1998. Identification of the second heparin-binding domain in human complement factor H. J. Immunol. 160, 3342–3348.

Blom, A.M., Bergström, F., Edey, M., Diaz-Torres, M., Kavanagh, D., Lampe, A., Goodship, J.A., Strain, L., Moghal, N., McHugh, M., Inward, C., Tomson, C., Frémeaux-Bacchi, V., Villoutreix, B.O., Goodship, T.H.J., 2008. A novel non-synonymous polymorphism (p.Arg240His) in C4b-binding protein is associated with atypical hemolytic uremic syndrome and leads to impaired alternative pathway cofactor activity. J. Immunol. 180, 6385–6391.

Caprioli, J., Bettinaglio, P., Zipfel, P.F., Amadei, B., Daina, E., Gamba, S., Skerka, C., Marziliano, N., Remuzzi, G., Noris, M., 2001. The molecular basis of familial hemolytic uremic syndrome: mutation analysis of factor H gene reveals a hot spot in short consensus repeat 20. J. Am. Soc. Nephrol. 12, 297–307.

Caprioli, J., Castelletti, F., Bucchioni, S., Bettinaglio, P., Bresin, E., Pianetti, G., Gamba, S., Brioschi, S., Daina, E., Remuzzi, G., Noris, M., 2003. Complement factor H mutations and gene polymorphisms in haemolytic uraemic syndrome: the C-257T, the A2089G and the G2881T polymorphisms are strongly associated with the disease. Hum. Mol. Genet. 12, 3385–3395.

Caprioli, J., Noris, M., Brioschi, S., Pianetti, G., Castelletti, F., Bettinaglio, P., Mele, C., Bresin, E., Cassis, L., Gamba, S., Porrati, F., Bucchioni, S., Monteferrante, G., Fang, C.J., Liszewski, M.K., Kavanagh, D., Atkinson, J.P., Remuzzi, G., 2006. For the international registry of recurrent and familial HUS/TTP Genetics of HUS: the impact of MCP CFH, and IF mutations on clinical presentation, response to treatment, and outcome. Blood 108, 1267–1279.

Delvaeye, M., Noris, M., De Vriese, A., Esmon, C.T., Esmon, N.L., Ferrell, G., Del-Favero, J., Plaisance, S., Claes, B., Lambrechts, D., Zoja, C., Remuzzi, G., Conway, E.M., 2009. Thrombomodulin mutations in atypical hemolytic-uremic syndrome. N. Engl. J. Med. 361, 345–357.

Dragon-Durey, M.A., Loirat, C., Cloarec, S., Macher, M.A., Blouin, J., Nivet, H., Weiss, L., Fridman, W.H., Frémeaux-Bacchi, V., 2005. Anti-factor H antibodies associated with atypical hemolytic uremic syndrome. J. Am. Soc. Nephrol. 16, 555–563.

Esparza-Gordillo, J., Goicoechea de Jorge, E., Buil, A., Carreras-Berges, L., López-Trascasa, M., Sánchez-Corral, P., Rodríguez de Córdoba, S., 2005. Predisposition to atypical hemolytic uremic syndrome involves the concurrence of different susceptibility alleles in the regulators of complement activation gene cluster in 1q32. Hum. Mol. Genet. 14, 703–712.

Ferreira, V.P., Pangburn, M.K., 2007. Factor H mediated cell surface protection from complement is critical for the survival of PNH erythrocytes. Blood 110, 2190–2192.

Józsi, M., Strobel, S., Dahse, H.M., Liu, W.S., Hoyer, P.F., Oppermann, M., Skerka, C., Zipfel, P.F., 2007. Anti factor H autoantibodies block C-terminal recognition function of factor H in hemolytic uremic syndrome. Blood 110, 1516–1518.

Karmali, M.A., Petric, M., Lim, C., Fleming, P.C., Steele, B.T., 1983. *Escherichia coli* cytotoxin, haemolytic-uraemic syndrome, and haemorrhagic colitis. Lancet 322, 1299–1300.

Karmali, M.A., Petric, M., Lim, C., Fleming, P.C., Arbus, G.S., Lior, H., 1985. The association between idiopathic hemolytic uremic syndrome and infection by verotoxin-producing *Escherichia coli*. J. Infect. Dis. 151, 775–782.

Kaplan, B.S., Chesney, R.W., Drummond, K.N., 1975. Hemolytic uremic syndrome in families. N. Engl. J. Med. 292, 1090–1093.

Kaplan, B.S., Meyers, K.E., Schulman, S.L., 1998. The pathogenesis and treatment of hemolytic uremic syndrome. J. Am. Soc. Nephrol. 9, 1126–1133.

Martínez-Barricarte, R., Goicoechea de Jorge, E., Montes, T., Layana, A.G., Rodríguez de Córdoba, S., 2008. Lack of association between polymorphisms in C4b-binding protein and atypical haemolytic uraemic syndrome in the Spanish population. Clin. Exp. Immunol. 155, 59–64.

Neumann, H.P., Salzmann, M., Bohnert-Iwan, B., Mannuelian, T., Skerka, C., Lenk, D., Bender, B.U., Cybulla, M., Riegler, P., Königsrainer, A., Neyer, U., Bock, A., Widmer, U., Male, D.A., Franke, G., Zipfel, P.F., 2003. Haemolytic uraemic syndrome and mutations of the factor H gene: a registry-based study of German speaking countries. J. Med. Genet. 40, 676–681.

Noris, M., Remuzzi, G., 2009. Atypical hemolytic-uremic syndrome. N. Engl. J. Med. 361, 1676–1687.

Oppermann, M., Baumgarten, H., Brandt, E., Gottsleben, W., Kurts, C., Götze, O., 1990. Quantitation of components of the alternative pathway of complement (APC) by enzyme-linked immunosorbent assays. J. Immunol. Methods 133, 181–190.

Pangburn, M.K., Schreiber, R.D., Müller-Eberhard, H.J., 1977. Human complement C3b inactivator: isolation, characterization, and demonstration of an absolute requirement for the serum protein β1H for cleavage of C3b and C4b in solution. J. Exp. Med. 146, 257–270.

Pangburn, M.K., 2002. Cutting edge: localization of the host recognition functions of complement factor H at the carboxyl-terminal: implications for hemolytic uremic syndrome. J. Immunol. 169, 4702–4706.

Richards, A., Buddles, M.R., Donne, R.L., Kaplan, B.S., Kirk, E., Venning, M.C., Tielemans, C.L., Goodship, J.A., Goodship, T.H.J., 2001. Factor H mutations in hemolytic uremic syndrome cluster in exons 18–20, a domain important for host cell recognition. Am. J. Hum. Genet. 68, 485–490.

Rodríguez de Córdoba, S., Esparza-Gordillo, J., Goicoechea de Jorge, E., Lopez-Trascasa, M., Sánchez-Corral, P., 2004. The human complement factor H: functional roles, genetic variations and disease associations. Mol. Immunol. 41, 355–367.

Sánchez-Corral, P., González-Rubio, C., Rodríguez de Córdoba, S., López-Trascasa, M., 2004. Functional analysis in serum from atypical hemolytic uremic syndrome patients reveals impaired protection of host cells associated with mutations in factor H. Mol. Immunol. 41, 81–84.

Sánchez-Corral, P., Melgosa, M., 2010. Advances in understanding the aetiology of atypical haemolytic uraemic syndrome. Br. J. Haematol. 150, 529–542.

Saunders, R.E., Goodship, T.H.J., Zipfel, P.F., Perkins, S.J., 2006. An interactive web database of factor H-associated hemolytic uremic syndrome mutations: insights into the structural consequences of disease-associated mutations. Hum. Mutat. 27, 21–30.
Scheiring, J., Rosales, A., Zimmerhackl, L.B., 2010. Clinical practice Today's understanding of the haemolytic uraemic syndrome. Eur. J. Pediatr. 169, 7–13.
Weiler, J.M., Daha, M.R., Austen, K.F., Fearon, D.T., 1976. Control of the amplification convertase of complement by the plasma protein β1H· Proc. Natl. Acad. Sci. U. S. A. 73, 3268–3272.
Whaley, K., Ruddy, S., 1976. Modulation of the alternative complement pathway by β1H globulin. J. Exp. Med. 144, 1147–1163.
Zipfel, P.F., Skerka, C., 1999. FHL-1/reconectin: a human complement and immune regulator with cell-adhesive function. Immunol. Today 20, 135–140.

Aurora kinase A-specific T-cell receptor gene transfer redirects T lymphocytes to display effective antileukemia reactivity

*Kozo Nagai,[1] *Toshiki Ochi,[1] Hiroshi Fujiwara,[1,2] Jun An,[1] Toshiaki Shirakata,[1] Junichi Mineno,[3] Kiyotaka Kuzushima,[4] Hiroshi Shiku,[5] J. Joseph Melenhorst,[6] Emma Gostick,[7] David A. Price,[7] Eiichi Ishii,[8] and Masaki Yasukawa[1,2]

[1]Department of Bioregulatory Medicine, Ehime University Graduate School of Medicine, Ehime, Japan; [2]Department of Cell Growth and Cancer Regulation, Ehime University Proteomedicine Research Center, Ehime, Japan; [3]Takara Bio Inc Center for Cell and Gene Therapy, Shiga, Japan; [4]Division of Immunology, Aichi Cancer Center, Aichi, Japan; [5]Department of Cancer Vaccine and Immuno-Gene Therapy, Mie University Graduate School of Medicine, Mie, Japan; [6]Hematology Branch, National Heart, Lung, and Blood Institute, National Institutes of Health, Bethesda, MD; [7]Department of Infection, Immunity and Biochemistry, Cardiff University School of Medicine, Cardiff, United Kingdom; and [8]Department of Pediatrics, Ehime University Graduate School of Medicine, Ehime, Japan

Aurora kinase A (AURKA) is overexpressed in leukemias. Previously, we demonstrated that AURKA-specific CD8$^+$ T cells specifically and selectively lysed leukemia cells, indicating that AURKA is an excellent target for immunotherapy. In this study, we examined the feasibility of adoptive therapy using redirected T cells expressing an HLA-A*0201–restricted AURKA$_{207-215}$-specific T-cell receptor (TCR). Retrovirally transduced T cells recognized relevant peptide-pulsed but not control target cells. Furthermore, TCR-redirected CD8$^+$ T cells lysed AURKA-overexpressing human leukemic cells in an HLA-A*0201–restricted manner, but did not kill HLA-A*0201$^+$ normal cells, including hematopoietic progenitors. In addition, AURKA$_{207-215}$-specific *TCR*-transduced CD4$^+$ T cells displayed target-responsive Th1 cytokine production. Finally, AURKA$_{207-215}$-specific *TCR*-transduced CD8$^+$ T cells displayed antileukemia efficacy in a xenograft mouse model. Collectively, these data demonstrate the feasibility of redirected T cell–based AURKA-specific immunotherapy for the treatment of human leukemia. (*Blood*. 2012;119(2):368-376)

Introduction

Aurora kinase A (AURKA) is a member of the serine-threonine kinase family that regulates mitotic cell division from G_2 through to M phase of the cell cycle.[1] The *AURKA* gene maps to chromosome region 20q13.2. AURKA is expressed at low levels in normal cells, including dividing cells, and overexpression of AURKA has clear oncogenic potential.[2,3] Indeed, the *AURKA* gene is overexpressed in various types of cancer,[4] including leukemias.[5,6] Furthermore, correlations between the genetic dysregulation of *AURKA* and susceptibility to cancer, disease status, and prognosis have been described.[4] In particular, *AURKA* gene overexpression correlates with genetic instability and poor differentiation of cancer cells.[7,8] As AURKA expression is tightly regulated in normal tissues and overexpression correlates with malignant transformation, small molecular inhibitors have been developed that selectively target this protein in various tumors. A number of such molecules are currently in early phase clinical trials and preliminary data are encouraging.[9-12]

The overexpression of AURKA in cancer cells, but not in normal tissues, makes it an attractive target for tumor immunotherapy. We have previously shown that testis is the only tissue that expresses detectable levels of AURKA, which suggests that this antigen behaves like cancer/testis antigens.[13] Based on these findings, we previously studied the immunotherapeutic potential of AURKA and identified an HLA-A*0201-restricted antigenic nonamer epitope derived from the kinase domain (residues 207-215). The AURKA$_{207-215}$ epitope (YLILEYAPL) was recognized by CD8$^+$ cytotoxic T lymphocytes (CTLs) generated in vitro.[6] Furthermore, leukemic cells endogenously expressing AURKA were killed by these CTLs, indicating that the cognate epitope is naturally processed and presented in the context of HLA-A*0201 at levels sufficient for immunotherapeutic applications. In addition, Kobayashi and colleagues have identified HLA-class II–restricted AURKA-derived pentadecamer epitopes to which they could generate CD4$^+$ helper T cells that expressed antitumor reactivity.[14]

Immunotherapeutic interventions based on tumor antigen-specific *T-cell receptor* (*TCR*) gene transfer to redirect the specificity of other T cells has shown clinical success in patients with advanced melanoma.[15] However, this approach is complicated by several potential problems: (1) on-target adverse events directed against normal tissues, especially when affinity-enhanced TCRs are used[16]; (2) issues related to chain mispairing between the introduced and endogenous *TCR* α/β genes; and (3) off-target adverse events because of inherent cross-reactivity of the introduced TCR.[17] Although various solutions have been explored to minimize TCR chain mispairing, all current approaches have intrinsic limitations. To this end, we have recently developed a unique vector system that simultaneously delivers *siRNA*s, which specifically down-regulate endogenous *TCR* expression, and a *siRNA*-resistant relevant *TCR* construct (si-*TCR* vector).[18] Furthermore, the likelihood of adverse events related to expression of the introduced TCR may be minimized by the selection of tumor-specific antigens or cancer/testis antigens, rather than tumor-associated antigens. Indeed, a recent clinical study reported that redirected T-cell therapy using NY-ESO-1–specific *TCR* gene

Submitted June 11, 2011; accepted October 13, 2011. Prepublished online as *Blood* First Edition paper, October 24, 2011; DOI 10.1182/blood-2011-06-360354.

*K.N. and T.O. contributed equally to this work.

An Inside *Blood* analysis of this article appears at the front of this issue.

The online version of this article contains a data supplement.

The publication costs of this article were defrayed in part by page charge payment. Therefore, and solely to indicate this fact, this article is hereby marked "advertisement" in accordance with 18 USC section 1734.

transfer displayed antitumor efficacy against metastatic melanoma and metastatic synovial cell sarcoma without obvious toxicities mediated by the transferred T cells.[19]

In this study, we examined the antileukemic efficacy and safety of redirected T cells using HLA-A*0201–restricted $AURKA_{207-215}$–specific *TCR* gene transfer both in vitro and in vivo. The data demonstrate the feasibility of this approach for the treatment of human leukemias.

Methods

Cells and cell lines

Approval for this study was obtained from the Institutional Review Board of Ehime University Hospital (Protocol 0909001 and 0909002). Written informed consent was obtained from all patients, healthy volunteers, and parents of cord blood donors in accordance with the Declaration of Helsinki. B-lymphoblastoid cell lines (B-LCLs) were established by transformation of peripheral blood B-lymphocytes with Epstein-Barr virus. GANMO-1 (HLA-$A2^+$), MEG01 (HLA-$A2^-$), MEG01-A2 (*HLA-A*0201* gene-transduced MEG01), OUN-1 (HLA-$A2^-$), and KAZZ (HLA-$A2^-$) leukemia cell lines were cultured in RPMI 1640 with 10% FCS, antibiotics, and L-glutamine. The artificial antigen-presenting cell line C1R-A2 (HLA-$A*0201^+$) was a kind gift from Dr A. John Barrett (National Heart, Lung, and Blood Institute, Bethesda, MD). The Jurkat/MA cell line (kindly provided by Prof Erik Hooijberg, Vrije Universiteit Medisch Centrum, Amsterdam, The Netherlands) is a Jurkat cell subclone that lacks endogenous TCR expression and stably expresses both the human *CD8α* gene (*hCD8α*) and an *NFAT-luciferase* gene construct for the detection of signaling via newly introduced TCRs.[20] PBMCs and bone marrow mononuclear cells (BMMCs) from leukemia patients and healthy volunteers, and cord blood mononuclear cells (CBMCs) from healthy donors, were isolated by density gradient centrifugation and stored in liquid nitrogen until use. $CD34^+$ cells from CBMCs were isolated using $CD34^+$ cell-isolating immunomagnetic beads (Miltenyi Biotec).

Synthetic peptides and HLA-A*0201/peptide tetrameric complexes

The HLA-A*0201–restricted $AURKA_{207-215}$ nonameric peptide (YLILEYAPL) was purchased from Thermo Electron (Greiner Bio-One). Biotin-tagged soluble HLA-A*0201/AURKA monomers were produced as previously described.[21] Fluorochrome-labeled tetrameric complexes were generated by conjugation to streptavidin-PE (Prozyme) at a molar ratio of 4:1.[22] HLA-A*0201 tetramers were also produced with the HIV-1 p17 Gag-derived peptide epitope SL9 (SLYNTVATL, residues 77-85) for control purposes.

Generation of an $AURKA_{207-215}$-specific CTL clone

A novel $AURKA_{207-215}$-specific CTL clone designated AUR-2 was generated as previously described.[23] Briefly, monocyte-derived dendritic cells (Mo-DCs) were generated from $CD14^+$ PBMCs using 10 ng/mL recombinant human IL-4 and 75 ng/mL recombinant human GM-CSF (R&D systems), then matured with 100 U/mL recombinant human TNF-α (Dainippon Pharmaceutical). $CD8^+$ T cells (1×10^5) were stimulated with 10^4 autologous mature $AURKA_{207-215}$ peptide-loaded (10μM) Mo-DCs in a 96-well round-bottomed plate. One week later, the $CD8^+$ T cells were restimulated similarly, and 10 U/mL recombinant human IL-2 (Roche) was added after a further 4 days. Thereafter, $CD8^+$ T cells were restimulated weekly with 10^5 autologous $AURKA_{207-215}$ peptide-pulsed (10μM) PBMCs treated with mitomycin-C (MMC; Kyowa Hakko). Epitope-dependent target cell cytotoxicity was examined using standard ^{51}chromium (^{51}Cr)–release assays.

ELISPOT

ELISPOT assays were conducted as previously described.[22] Briefly, 96-well flat-bottomed MultiScreen-HA plates with a nitrocellulose base (Millipore) were coated overnight at 4°C with 10 μg/mL anti-IFN-γ monoclonal antibody (mAb; R&D Systems). After washing with PBS, cultured $CD8^+$ T cells were stimulated with 5×10^4 $AURKA_{207-215}$ peptide-pulsed (1μM) or unpulsed C1R-A2 cells/well for 20 hours at 37°C in a 5% CO_2 atmosphere. Subsequently, the wells were vigorously washed with PBS/0.05% tween 20 and incubated with polyclonal rabbit anti–IFN-γ Ab (Endogen) for 90 minutes at room temperature. The wells were then washed again and incubated for 90 minutes with peroxidase-conjugated goat anti–rabbit IgG Ab (Zymed). Spots were visualized by the addition of 100 μL substrate, comprising 0.1M sodium acetate buffer (pH 5.0) containing 3-amino-9-ethylcarbazole (Sigma-Aldrich) and 0.015% H_2O_2, for 40 minutes at room temperature and counted under a light microscope.

Cloning of full-length *TCR* α and β chain genes from the AUR-2 CTL clone and retroviral vector construction

Total RNA was extracted from the HLA-A*0201–restricted $AURKA_{207-215}$-specific CTL clone AUR-2 using the FastPure RNA Kit (Takara Bio) according to the manufacturer's instructions. Full-length *TCR* α and β genes were cloned as previously described.[24] Briefly, cDNA was amplified using a 5′-RACE primer and 3′-constant region primers as follows: (1) 5′-TCAGCTGGACCACAGCCGCAGCGT-3′ for TCR Cα; (2) 5′-TCAGAAATCCTTTCTCTTGAC-3′ for TCR Cβ1; and (3) 5′-CTAGCCTCTGGAATCCTTTCTCTT-3′ for TCR Cβ2. The conditions for PCR were: one cycle at 94°C for 3 minutes, followed by 30 cycles at 94°C for 40 seconds, 58°C for 40 seconds and 72°C for 1 minute, with a final extension phase at 72°C for 5 minutes. Each *TCR* α and β chain amplicon was cloned into the pMD20 TA cloning vector (Takara Bio), and sequenced using the BigDye Terminator v3.1 Cycle Sequencing Kit (Applied Biosystems) and an ABI 3730xl sequencer (Applied Biosystems). Full-length *TCR* α and β genes were then cloned into the bicistronic pMS3 retroviral vector, which is a pME1-5 derivative that contains the murine stem cell virus (MSCV) LTR (Takara Bio) in place of the 3′LTR (pMS3-*AURKA-TCR*, Figure 1). Ecotropic retrovirus particles were obtained by transient transfection of HEK293 T cells with the TCR construct and helper plasmids (pGP vector and pE-eco vector; Takara Bio). GaLV-pseudotyped retrovirus particles were obtained by consecutive transfection into PG13 cells. The pMS3-*AURKA-TCR* GaLV-pseudotyped retroviruses were used for AURKA-specific *TCR* α and β gene transduction.

Transduction of $AURKA_{207-215}$-specific *TCR genes*

Jurkat/MA cells and healthy donor T cells were genetically modified to express the AURKA-specific TCR using RetroNectin (Takara Bio) as previously described.[18] Briefly, 1×10^6 healthy donor T cells per well in GT-T503 (Takara Bio) with 5% human serum, 0.2% human albumin, 50 U/mL recombinant human IL-2 (R&D Systems), 5 ng/mL recombinant human IL-7 (R&D Systems), 10 ng/mL recombinant human IL-15 (PeproTech Inc), and 100 ng/mL recombinant human IL-21 (Shenandoah Biotechnology Inc) were added on day 1 to a 24-well culture plate pretreated with antihuman CD3 mAb (BioLegend). Jurkat/MA cells were cultured in IMDM with 8% FCS and 50 μg/mL hygromycin B (Invitrogen). On day 3, cultured T cells or Jurkat/MA cells were transferred on to a retrovirus-preloaded RetroNectin-coated 24-well plate, centrifuged at 2000*g* for 2 hours and rinsed with PBS. Cells were then applied to the retrovirus-preloaded RetroNectin-coated 24-well plate again for the second transduction. AURKA-specific *TCR*-transduced T cells were stimulated weekly with MMC-treated C1R-A2 cells loaded with $AURKA_{207-215}$ peptide (1μM) for further functional experiments.

Flow cytometric analysis

The AUR-2 CTL clone expresses the *TRBV10-3* gene, denoted in IMGT nomenclature.[25] This corresponds to TCR Vβ12 in the Arden nomenclature.[26] Accordingly, anti-TCR Vβ12 mAb was used to detect $AURKA_{207-215}$-specific *TCR*-transduced cells. After 4 to 6 days, transduced cells were analyzed by flow cytometry using anti-TCR Vβ12-FITC (Beckman Coulter), anti-CD8–FITC (BD Biosciences) or anti-CD8–PE (BioLegend), and HLA-A*0201/$AURKA_{207-215}$ tetramer-PE (only with anti-CD8–FITC).

Intracellular expression of Foxp3 and $AURKA_{207-215}$–responsive IFN-γ production by $AURKA_{207-215}$–specific *TCR*-transduced $CD4^+$ T cells were analyzed using anti–Foxp3-PE (e-Bioscience) and anti–IFN-γ–FITC (BD Biosciences). Data were acquired using a FACS Calibur flow cytometer and analyzed with either Cell Quest (BD Biosciences) or FlowJo Version 7.2.2 software (TreeStar Inc).

CFSE dilution assay

To measure epitope-responsive proliferation of $AURKA_{207-215}$–specific *TCR*-transduced $CD8^+$ T cells in the presence or absence of similarly redirected $CD4^+$ T cells, $CD8^+$ T cells were labeled with CFSE (Molecular Probe Inc) as described previously.[27] After 3 days, CFSE dilution within the $CD8^+$ T-cell population was assessed by flow cytometry.

Epitope-responsive luciferase production by $AURKA_{207-215}$–specific *TCR*-transduced Jurkat/MA cells

To verify the functionality of the cloned $AURKA_{207-215}$–specific *TCR* α and β chains, we used the TCR^- Jurkat/MA cell line, which stably expresses *hCD8α* and an *NFAT-luciferase* reporter gene (Jurkat/MA/CD8α/luc), as follows. pMS3-*AURKA-TCR* was retrovirally transduced into Jurkat/MA/CD8α/luc cells. Cells expressing TCR Vβ12 were isolated for functional analysis. Briefly, HLA-A*0201$^+$ B-LCL cells were loaded with titrated doses of $AURKA_{207-215}$ peptide or the irrelevant SL9 peptide (10μM; HIV-1 p17 Gag, residues 77-85) and used to stimulate 8×10^5 *TCR* gene-modified Jurkat/MA/CD8α/luc cells (effector:target ratio 2:1) for 12 hours. The cells were then lysed and subjected to luciferase assay using the PicaGene-Dual-SeaPansy Kit (TOYOinki) according to manufacturer's instructions. Luciferase activity was measured using a Lumicounter700 (MicrotecNition).

IFN-γ secretion assay

$AURKA_{207-215}$–specific *TCR*-transduced $CD4^+$ or $CD8^+$ T cells (5×10^5) were incubated with 10^5 $AURKA_{207-215}$ peptide-pulsed (1μM) or unpulsed C1R-A2 cells for 24 hours. For the inhibition assay, cells were cultured in the presence of either an anti-HLA class I framework mAb (w6/32; ATCC) or a control anti–HLA-DR mAb (L243; ATCC). Cytokine production patterns were assessed using a bead-based immunoassay kit (Becton Dickinson). IFN-γ in the culture supernatant was measured using an ELISA kit (Pierce) according to the manufacturer's instructions. Streptavidin-HRP was used for color development, and luminointensity was measured using IMMUNO-MINI (NJ-2300; Microtec).

Cytotoxicity assay

Standard ^{51}Cr release assays were performed as previously described.[28] Briefly, 10^4 unpulsed or peptide-pulsed target cells were labeled with ^{51}Cr ($Na_2{}^{51}CrO_4$; MP Bio Japan) and incubated at various ratios with effector cells in 200 μL of culture medium in 96-well round-bottomed plates. To assess HLA class I restriction, target cells were incubated with 10 μg/mL w6/32 mAb or the control L243 mAb for 1 hour, then incubated with effector cells for 5 hours. After incubation, 100 μL supernatant was collected from each well to measure ^{51}Cr release. The percentage specific lysis was calculated as: (experimental release cpm − spontaneous release cpm)/(maximal release cpm − spontaneous release cpm) × 100 (%).

Quantitative analysis of *AURKA* mRNA expression

Quantitative real-time PCR (qRT-PCR) for *AURKA* mRNA was performed as described previously.[6] Briefly, total RNA was extracted using an RNeasy Mini Kit (QIAGEN) and cDNA was synthesized. qRT-PCRs for *AURKA* mRNA (Hs00269212_ml) and glyceraldehyde-3-phosphate dehydrogenase (*GAPDH*) mRNA (4326317E) as an internal control were performed using the TaqMan Gene Expression assay (Applied Biosystems) in accordance with the manufacturer's instructions and an ABI Prism 7700 Sequence Detection System (Applied Biosystems). The expression level of *AURKA* mRNA was corrected by reference to that of *GAPDH* mRNA, and the relative amount of *AURKA* mRNA in each sample was calculated by the comparative ΔCt method.

AURKA protein expression analysis by Western blotting

For the analysis of protein expression, Western blotting was performed as described previously.[6] Briefly, cell lysates were subjected to 10% SDS-PAGE (e-PAGEL, ATTO) and blotted onto PVDF membranes (Bio-Rad Laboratories). The blots were incubated first with anti-AURKA mouse mAb (Abcam), then with HRP-conjugated anti–mouse IgG (GE Healthcare). The probed proteins were visualized using an enhanced chemiluminescence system (GE Healthcare). Subsequently, the blotted membranes were stripped and reprobed with anti–β-actin mouse mAb (Sigma-Aldrich) to confirm equivalent protein loading between samples.

Antileukemia effect of $AURKA_{207-215}$–specific *TCR*-transduced T cells in xenograft mouse models

All in vivo experiments were approved by the Ehime University animal care committee. For the Winn assay, 5×10^6 GANMO-1 cells and 2.5×10^7 $AURKA_{207-215}$–specific *TCR* gene-transduced or non–gene-modified $CD8^+$ T cells were inoculated per mouse (n = 4 per group). The cells were suspended in 300 μL PBS and injected subcutaneously into the left flank of NOG mice (Non-Obese Diabetic/Severe Combined Immuno-Deficiency/IL-2 receptor γ-chain allelic mutation; *NOD*/Shi-*scid*/IL-2R γ^{null})[29] aged 5-6 weeks (Central Institute for Experimental Animals). Mice were subsequently injected intravenously with either 5×10^6 $AURKA_{207-215}$–specific *TCR* gene-modified cells, AUR-2 cells or unmodified $CD8^+$ T cells, as per the initial inoculation, on a weekly basis for a total of 5 infusions. Tumor size was measured every 5 days until the mice died or were euthanized because of tumor progression.

For adoptive transfer experiments, NOG mice aged 9 weeks were similarly inoculated with 5×10^6 of GANMO-1 cells. Intravenous administration of either 5×10^6 $AURKA_{207-215}$–specific *TCR* gene-transduced or non–gene-modified $CD8^+$ T cells commenced on the same day (day 0), and was continued on a weekly basis thereafter until the mice died or were euthanized because of tumor progression.

Statistical analysis

The paired *t* test was used to assess differences between groups; a *P* value $< .05$ was considered significant.

Results

Generation of a novel HLA-A*0201–restricted $AURKA_{207-215}$–specific CTL clone (AUR-2) and retroviral expression of the full-length *TCR* α and β genes

Characteristics of the newly established HLA-A*0201-restricted $AURKA_{207-215}$–specific CTL clone (AUR-2) are shown in Figure 1. AUR-2 was stained uniformly with the HLA-A*0201/$AURKA_{207-215}$ tetramer, but not with the irrelevant HLA-A*0201/Gag_{77-85} tetramer (Figure 1A). In cytotoxicity assays, AUR-2 displayed moderate levels of functional sensitivity in response to cognate peptide (Figure 1B). Epitope-dependent production of IFN-γ was confirmed in ELISPOT assays (Figure 1C). Peptide specificity and HLA restriction were further demonstrated in cytotoxicity assays with different target cells (Figure 1D). In addition, AUR-2 lysed the HLA-A*0201$^+$ leukemia cell line GANMO-1, which overexpresses *AURKA* mRNA, but not the HLA-A*0201$^-$ negative cell lines MEG01 and K562, both of which also express *AURKA* mRNA at high levels (Figure 1E). The rearranged *TCR* α and β genes of AUR-2 were sequenced and found to comprise the germ line gene segments *TRAV3/TRAJ20/TRAC* and *TRBV10-3/TRBJ1-1/TRBC1*, respectively; both full-length genes were cloned into a novel bicistronic retroviral vector (Figure 1F).

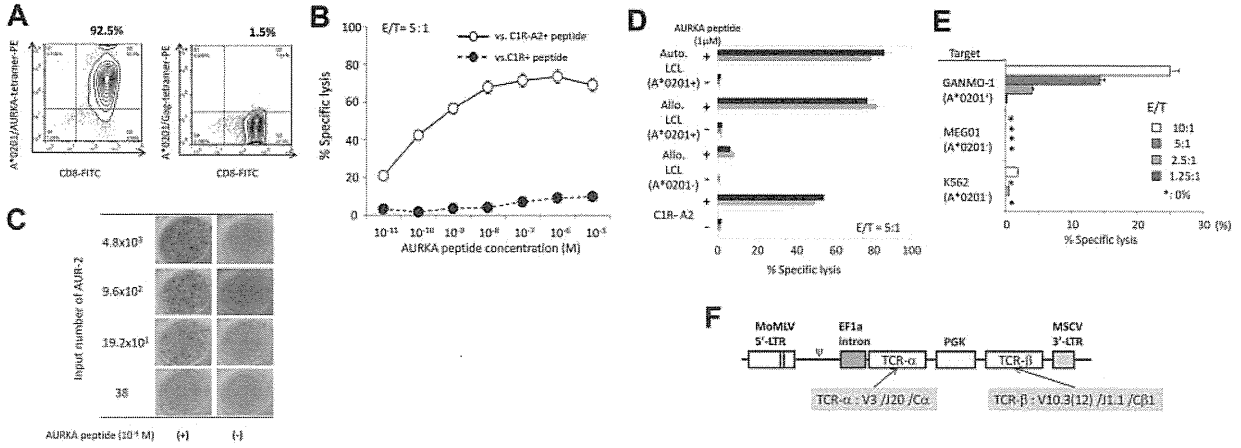

Figure 1. Characteristics of the AURKA$_{207\text{-}215}$–specific CTL clone AUR-2. (A) Representative flow cytometry plots showing staining of AUR-2 with the HLA-A*0201/AURKA$_{207\text{-}215}$ tetramer (left) and the irrelevant HLA-A*0201/Gag$_{77\text{-}85}$ tetramer (negative control; right). (B) The cyotoxic activity of AUR-2 was measured in ^{51}Cr-release assays against C1R-A2 or C1R (negative control) cells loaded with a range of AURKA$_{207\text{-}215}$ peptide concentrations as indicated. E/T indicates effector:target ratio. (C) IFN-γ ELISPOT assays were conducted using C1R-A2 target cells loaded with 1 μM AURKA$_{207\text{-}215}$ peptide and AUR-2 CTL at different input numbers as shown. (D) ^{51}Cr-release assays were conducted using AUR-2 CTL with unpulsed or AURKA$_{207\text{-}215}$ peptide-pulsed (1 μM) HLA-A*0201$^+$ autologous or allogeneic B-LCLs, C1R-A2 cells or HLA-A*0201$^-$ allogeneic B-LCLs as indicated. E/T indicates effector:target ratio. (E) The cytotoxic activity of AUR-2 CTL against the indicated leukemia cell lines was measured in ^{51}Cr-release assays. GANMO-1, HLA-A*0201$^+$; MEG01 and K562, HLA-A*0201$^-$. Expression of *AURKA* mRNA and AURKA protein in these leukemia cell lines is shown in supplemental Figure 2. E/T indicates effector:target ratio. (F) Construction of a novel retroviral vector encoding full-length AURKA–specific *TCR* α and β genes derived from AUR-2. MoMLV indicates Moloney murine leukemia virus; LTR, long terminal repeat; EF1a, elongation factor 1a; PGK, phosphoglycerate kinase promoter; and MSCV, murine stem cell virus. Error bars represent SDs.

Functional reconstitution of the AURKA$_{207\text{-}215}$–specific TCR heterodimer in Jurkat/MA cells

To validate the functionality of the cloned *TCR* genes, both chains were expressed in the TCR$^-$ cell line Jurkat/MA/CD8α/luc, which contains a luciferase reporter gene to monitor TCR signaling (Figure 2A). AUR-2*TCR*–transduced, Vβ12-selected Jurkat/MA/CD8α/luc cells (Figure 2B) were incubated with C1R-A2 cells pulsed with a range of AURKA$_{207\text{-}215}$ peptide concentrations, then assayed for luciferase activity. The *TCR* gene-modified Jurkat/MA/CD8α/luc cells produced luciferase in response to stimulation with AURKA$_{207\text{-}215}$ peptide-loaded C1R-A2 cells in a dose-dependent manner (Figure 2C). Compared with the parental AUR-2 CTL clone (Figure 1B), the *TCR*-transduced Jurkat/MA cells displayed low levels of peptide sensitivity. To address this functional discrepancy, we assessed cell-surface expression of TCR α/β, CD3, CD8α, CD11a, and CD28 (supplemental Figure 1, available on the *Blood* Web site; see the Supplemental Materials link at the top of the online article). The *TCR*-transduced Jurkat/MA cells expressed lower surface levels of TCR α/β, CD3 and CD8α compared with both similarly activated normal CD8$^+$ T cells and the parental AUR-2 CTL clone. Furthermore, CD11a and CD28 were almost absent from the transfectant cells. These findings may explain the observed differences in functional sensitivity between AUR-2 *TCR*-transduced Jurkat/MA cells and the parental CTL clone.

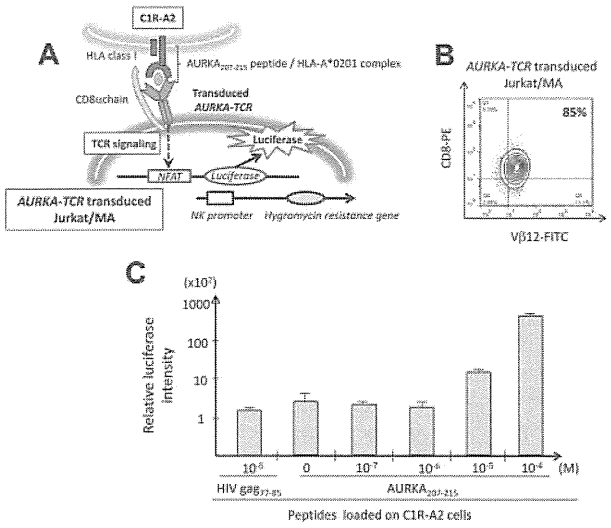

Figure 2. Functional retroviral expression of the AURKA$_{207\text{-}215}$–specific TCR. (A) Schematic representation of the luciferase assay using AURKA$_{207\text{-}215}$–specific *TCR*-transduced Jurkat/MA cells. NFAT indicates nuclear factor activated T cells; and NK, natural killer. (B) AURKA$_{207\text{-}215}$–specific *TCR*-transduced Jurkat/MA cells express Vβ12 but label poorly with cognate tetramer (data not shown), probably because of the low levels of surface CD8α expression. (C) AURKA$_{207\text{-}215}$–specific *TCR*-transduced Jurkat/MA cells were stimulated with peptide-pulsed C1R-A2 cells as shown and subjected to luciferase assay. Error bars represent SDs.

AURKA$_{207\text{-}215}$–specific *TCR* gene-transduced CD8$^+$ T cells exert antileukemia reactivity in vitro

Next, the AURKA$_{207\text{-}215}$–specific *TCR* was retrovirally introduced into normal CD8$^+$ T cells. Transduction efficiency determined by Vβ12 staining of *TCR* gene-modified T cells was 50%-70% (data not shown), and 20%-25% of the Vβ12$^+$ cells stained with the HLA-A*0201/AURKA$_{207\text{-}215}$ tetramer (Figure 3A). Isolated Vβ12$^+$ AURKA$_{207\text{-}215}$–specific *TCR* gene-transduced CD8$^+$ T cells displayed similar antigen sensitivity to the parental AUR-2 CTL clone (Figure 3B-C). Notably, however, the AURKA$_{207\text{-}215}$–specific *TCR* transductants produced higher quantities of IFN-γ in response to the same peptide-pulsed C1R-A2 targets (Figure 3C). On the basis of these observations, further experiments were carried out using these AURKA$_{207\text{-}215}$–specific *TCR* gene transfectants.

AURKA$_{207\text{-}215}$–specific *TCR*-transduced CD8$^+$ T cells displayed HLA class I–restricted, peptide-dependent IFN-γ production (Figure 3D), and target epitope–specific cytotoxic activity (Figure 3E). Furthermore, these redirected CD8$^+$ T cells selectively lysed the HLA-A*0201$^+$ leukemia cell line GANMO-1, which overexpresses AURKA, but not the HLA-A*0201$^-$ leukemia cell lines, MEG01, KAZZ, and OUN-1, which also overexpress AURKA (Figure 4A, supplemental Figure 2). In contrast,

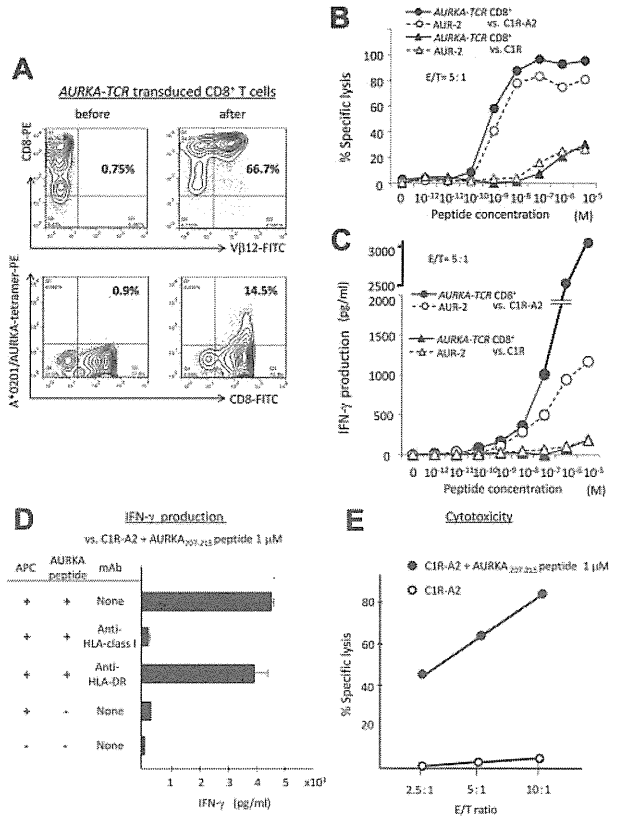

Figure 3. AURKA$_{207-215}$–specific *TCR*-transduced CD8$^+$ T cells display epitope-specific functionality. (A) Representative flow cytometry plots showing staining of AURKA$_{207-215}$–specific *TCR*-transduced CD8$^+$ T cells with anti-TCR Vβ12 mAb and HLA-A*0201/AURKA$_{207-215}$ tetramer. (B) The same AURKA$_{207-215}$ *TCR*-transduced CD8$^+$ T cells shown in panel A were tested in ^{51}Cr-release assays against C1R (negative control) and C1R-A2 cells pulsed with the indicated concentrations of AURKA$_{207-215}$ peptide. The parental AUR-2 CTL clone was tested in parallel. E/T indicates effector:target ratio. (C) IFN-γ production by AURKA$_{207-215}$–specific *TCR*-transduced CD8$^+$ T cells was measured in a similar format to that described for panel B. (D) Effects of HLA class I and class II blockade on the production of IFN-γ by AURKA$_{207-215}$–specific *TCR*-transduced CD8$^+$ T cells stimulated with cognate peptide-loaded (1 μM) C1R-A2 cells. (E) Cytotoxic activity of AURKA$_{207-215}$–specific *TCR*-transduced CD8$^+$ T cells against unpulsed or cognate peptide-loaded (1 μM) C1R-A2 cells as a function of effector:target (E/T) ratio. Error bars represent SDs.

HLA-A*0201$^+$ PBMCs (n = 3), PHA-stimulated lymphoblasts representing highly mitotic normal cells (n = 3), and normal cord blood CD34$^+$ cells (CB-CD34$^+$cells; n = 2) were not lysed by these AURKA$_{207-215}$–specific *TCR* transductants (Figure 4B). *AURKA* mRNA expression relative to K562 for each group (mean ± SD) was 0.02 ± 0.008 for PBMCs, 0.25 ± 0.005 for PHA-lymphoblasts and 0.21 ± 0.09 for CB-CD34$^+$ cells, which indicated relatively low expression levels of *AURKA* mRNA among these cells compared with K562. The cytotoxic activity of AURKA$_{207-215}$–specific *TCR*-transduced CD8$^+$ T cells against GANMO-1 and cognate peptide-loaded B-LCLs was significantly diminished by an anti-HLA class-I mAb but not by an anti–HLA-DR mAb (Figure 4C-D). To confirm recognition of the endogenously processed AURKA$_{207-215}$ epitope in the context of HLA-A*0201 expressed by leukemia cells, we retrovirally transduced the *HLA-A*0201* gene into MEG01 cells (MEG01-A2; Figure 4E). Parental MEG01 cells do not express HLA-A*0201, but abundantly overexpress both *AURKA* mRNA and AURKA protein (supplemental Figure 2). Compared with MEG01, MEG01-A2 were susceptible to the cytotoxic effects of AURKA$_{207-215}$–specific *TCR*-transduced CD8$^+$ T cells (Figure 4F). Collectively, these data indicate that the antileukemia reactivity mediated by AURKA$_{207-215}$–specific *TCR*-transduced CD8$^+$ T cells occurs through the recognition of endogenously processed and presented AURKA$_{207-215}$ peptide in the context of HLA-A*0201 on the surface of leukemia cells.

Next, the antileukemia reactivity mediated by these redirected AURKA$_{207-215}$–specific CD8$^+$ T cells was tested against freshly isolated leukemia cells in vitro (Figure 5). *AURKA* mRNA was overexpressed in all 6 leukemia samples as determined by qRT-PCR. Leukemia cells isolated from HLA-A*0201$^+$ patients (1-3), but not HLA-A*0201$^-$ patients (4-6) were lysed by the AURKA$_{207-215}$–specific *TCR*-transduced CD8$^+$ T cells. Thus, our data show that the AUR-2 TCR confers AURKA$_{207-215}$ specificity to donor CD8$^+$ T cells transduced with both TCR chains, and that normal cells, including actively cycling cells and hematopoietic progenitor cells, are not lysed by these redirected T cells.

AURKA$_{207-215}$–specific *TCR*-transduced CD4$^+$ T cells respond to cognate antigen

Next, we examined antigen reactivity in isolated populations of Vβ12$^+$ AURKA$_{207-215}$–specific *TCR*-transduced CD4$^+$ T cells (Figure 6A). AURKA$_{207-215}$–specific *TCR*-transduced CD4$^+$ T cells successfully produced IFN-γ in response to stimulation with AURKA$_{207-215}$ peptide-loaded C1R-A2 cells; this response was substantially reduced by HLA class I blockade, and a partial response reduction was also observed with HLA class II blockade (Figure 6B). These redirected CD4$^+$ T cells did not express Foxp3, which is a key molecular signature of regulatory T cells (supplemental Figure 3A), and the cognate antigen-specific proliferative response of AURKA$_{207-215}$–specific *TCR*-transduced CD8$^+$ T cells was actually enhanced in the presence of redirected CD4$^+$ T cells but not in the presence of non–gene-modified CD4$^+$ T cells (supplemental Figure 3B). Furthermore, AURKA$_{207-215}$–specific *TCR*-transduced CD4$^+$ T cells produced significant amounts of IL-2, TNF-α, and IFN-γ, but not IL-4 or IL-10 (supplemental Figure 4).

These observations suggest that AURKA$_{207-215}$–specific *TCR*-transduced CD4$^+$ T cells might be able to function as epitope-specific Th1 helper T cells, and that the interaction between T cell–expressed CD4 and target cell-expressed HLA class II molecules facilitates HLA class I–restricted AURKA$_{207-215}$–specific IFN-γ production.

AURKA$_{207-215}$–specific *TCR*-transduced CD8$^+$ T cells exhibit antileukemia reactivity in vivo

The in vivo antileukemia reactivity of AURKA$_{207-215}$–specific *TCR*-transduced CD8$^+$ T cells was assessed using the Winn assay and a therapeutic adoptive transfer model.

In the Winn assay, NOG mice were initially coinjected with GANMO-1 cells (5×10^6) and either 2.5×10^7 AURKA$_{207-215}$-specific *TCR* gene-modified or non–gene-modified CD8$^+$ T cells; 5 weekly infusions of the respective CD8$^+$ T-cell populations (5×10^6 cells per infusion) were subsequently administered. Treatment with AURKA$_{207-215}$–specific *TCR*-transduced CD8$^+$ T cells completely prohibited the engraftment and growth of inoculated leukemia cells for more than 2 months (Figure 7A), and significantly prolonged survival (Figure 7B). Similar results were obtained with AUR-2 cells in a parallel regimen (supplemental Figure 5). In contrast, non–gene-modified CD8$^+$ T cells did not prohibit leukemia growth. In a therapeutic adoptive transfer model, intravenously injected AURKA$_{207-215}$–specific *TCR*-transduced

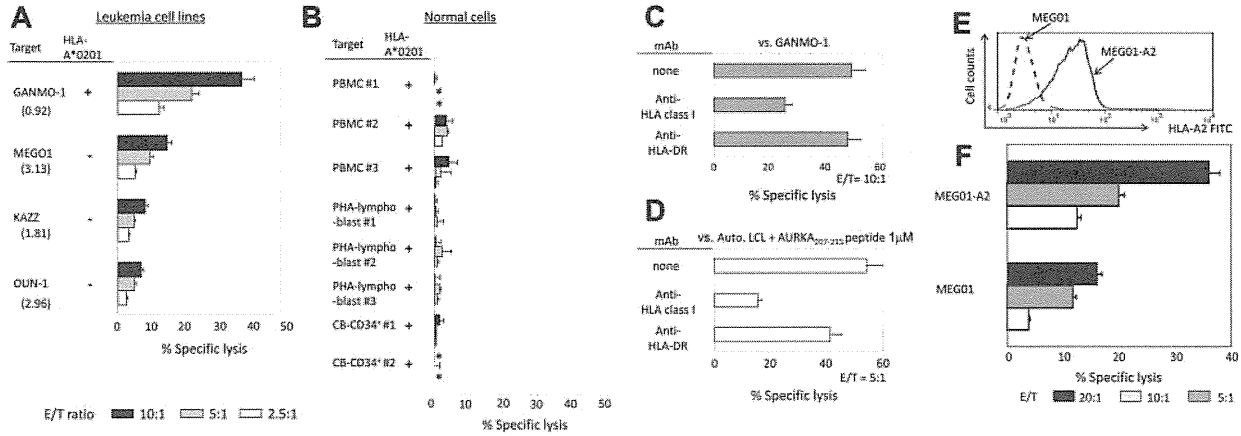

Figure 4. AURKA$_{207-215}$–specific *TCR*-transduced CD8$^+$ T cells can distinguish leukemia cells from normal cells on the basis of AURKA expression levels. (A) AURKA$_{207-215}$–specific *TCR*-transduced CD8$^+$ T cells exhibit antileukemia reactivity in an HLA-A*0201-dependent fashion. The HLA-A*0201$^+$ leukemia cell line GANMO-1 was lysed by AURKA$_{207-215}$–specific *TCR*-transduced CD8$^+$ T cells as a function of effector:target (E/T) ratio; no significant lysis was observed with the HLA-A*0201$^-$ leukemia cells lines MEG01, KAZZ and OUN-1. All of the tested leukemia cell lines overexpress *AURKA* mRNA; numbers in parentheses indicate *AURKA* mRNA expression relative to K562, and correlations with AURKA protein expression are shown in supplemental Figure 2. (B) The same AURKA$_{207-215}$–specific *TCR*-transduced CD8$^+$ T cells used in panel A at the same E/T ratios were tested in ^{51}Cr-release assays for potentially damaging effects against normal cells. No significant lysis was observed with HLA-A*0201$^+$ PBMCs (n = 3), PHA-lymphoblasts representing normal mitotic cells (n = 3) or normal cord blood–derived CD34$^+$ cells (CB-CD34$^+$) encompassing normal hematopoietic progenitor cells (n = 2). *AURKA* mRNA expression relative to K562 was 0.02 ± 0.008 for PBMCs, 0.25 ± 0.005 for PHA-lymphoblasts and 0.21 ± 0.09 for CB-CD34$^+$ cells (* indicates less than detectable). (C) Effects of HLA class I and class II blockade on the cytotoxic activity of AURKA$_{207-215}$–specific *TCR*-transduced CD8$^+$ T cells against GANMO-1 leukemia cells. E/T, effector:target ratio. (D) As for panel C, showing the effects of HLA class I and class II blockade on the lysis of autologous B-LCLs loaded with AURKA$_{207-215}$ peptide (1μM). (E) Flow cytometric confirmation of HLA-A*0201 expression by MEG01-A2 cells. (F) Enhanced lysis of MEG01-A2 cells relative to parental MEG01 cells by AURKA$_{207-215}$–specific *TCR*-transduced CD8$^+$ T cells confirms recognition of endogenously processed AURKA$_{207-215}$ peptide presented in the context of HLA-A*0201. E/T indicates effector:target ratio. Error bars represent SDs.

CD8$^+$ T cells, but not non–gene-modified CD8$^+$ T cells, significantly suppressed the growth of inoculated leukemia cells in vivo ($P < .02$; Figure 7C). Statistically significant tumor suppression was achieved on day 65, after 10 adoptive infusions. Thereafter, all mice (n = 4) treated with non–gene-modified CD8$^+$ T cells died by day 85. 2 mice treated with AURKA$_{207-215}$–specific *TCR*-transduced CD8$^+$ T cells died from other causes (1 on day 45 and 1 on day 70); the other 2 mice in this group survived longer than 90 days and were finally euthanized because of disease progression. Collectively, these observations indicate that AURKA$_{207-215}$–specific *TCR*-transduced CD8$^+$ T cells exhibit antileukemia reactivity in vivo.

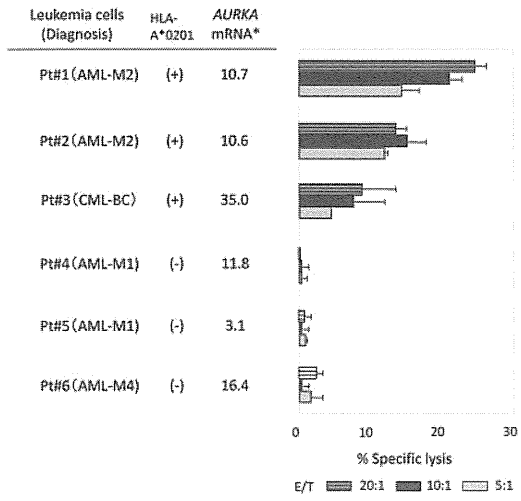

Figure 5. AURKA$_{207-215}$–specific *TCR*-transduced CD8$^+$ T cells kill freshly isolated leukemia cells in vitro. Freshly isolated HLA-A*0201$^+$ (n = 3) or HLA-A*0201$^-$ (n = 3) acute or chronic myeloid leukemia cells overexpressing *AURKA* mRNA were used as targets in ^{51}Cr-release assays with AURKA$_{207-215}$–specific *TCR*-transduced CD8$^+$ T cells at the indicated effector:target (E/T) ratios. AML, acute myeloid leukemia; BC, blast crisis; CML, chronic myeloid leukemia. M1, M2, and M4 refer to French-American-British classification subtypes (* indicates the expression of *AURKA* mRNA relative to the mean expression levels across 5 PBMC samples from healthy donors was determined by qRT-PCR and calculated using the comparative ΔCt method). Error bars represent SDs.

Discussion

In the setting of hematologic malignancies, *TCR* gene therapy targeting WT1 in leukemia,[30] and *chimeric antigen receptor* (*CAR*) gene therapy targeting CD33 in myeloid leukemias[31] and CD19, CD20, CD22, CD30, and the receptor tyrosine kinase-like orphan receptor 1 (ROR1) in B-cell malignancies,[32-38] are currently being investigated in preclinical studies or in early phase clinical trials.

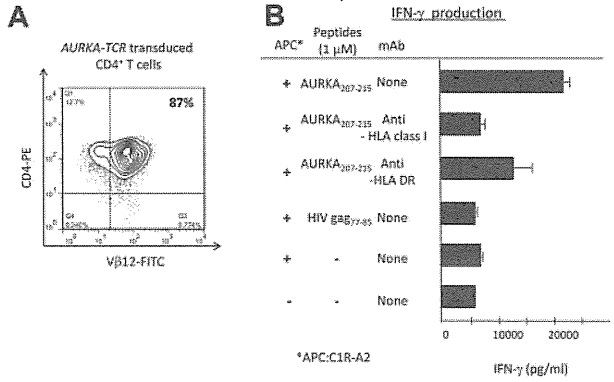

Figure 6. AURKA$_{207-215}$–*TCR* transduced CD4$^+$ T cells display antigen-specific Th1 cytokine production. (A) A representative flow cytometry plot showing surface Vβ12 expression by AURKA$_{207-215}$–specific *TCR*-transduced CD4$^+$ T cells. (B) *AURKA*$_{207-215}$–*TCR* transduced CD4$^+$ T cells produce IFN-γ in response to cognate peptide-loaded (1μM) C1R-A2 cells; unpulsed or irrelevant (HIV p17 Gag SL9) peptide-pulsed C1R-A2 cells were used as negative controls. Cognate antigen-specific IFN-γ production was reduced to background levels in the presence of anti-HLA class I blocking mAb and inhibited in the presence of anti-HLA class II blocking mAb. APC, antigen-presenting cell. Error bars represent SDs.

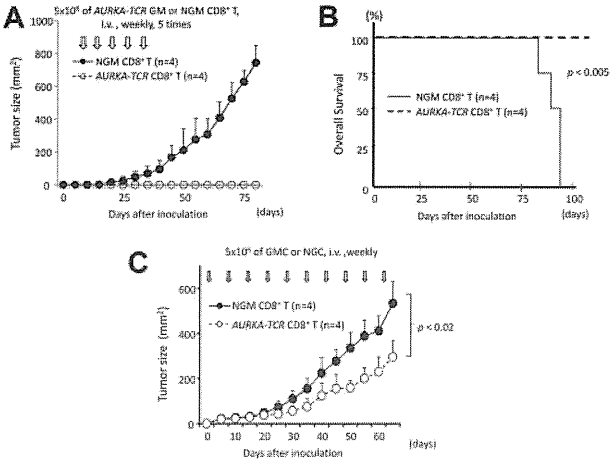

Figure 7. AURKA$_{207-215}$–specific *TCR*-transduced CD8$^+$ T cells mediate antileukemia reactivity in vivo. (A) Winn assay: tumor suppression curve. NOG mice were coinjected with GANMO-1 cells (5×10^6) and either 2.5×10^7 AURKA$_{207-215}$–specific *TCR* gene-modified (*AURKA-TCR*) or non–gene-modified (NGM) CD8$^+$ T cells (n = 4 group). Subsequently, 5 weekly infusions of the respective CD8$^+$ T-cell populations (5×10^6 cells per infusion) were administered intravenously. Tumor growth was monitored every 5 days. (B) Winn assay: survival curve. Treatment with AURKA$_{207-215}$–specific *TCR* gene-modified (*AURKA-TCR*) CD8$^+$ T cells significantly prolonged survival ($P < .005$). (C) Therapeutic adoptive transfer model. NOG mice (n = 4 per group) were inoculated with 5×10^6 of GANMO-1 cells. Intravenous administration of either 5×10^6 AURKA$_{207-215}$–specific *TCR* gene-modified (*AURKA-TCR*) or non–gene-modified (NGM) CD8$^+$ T cells commenced on the same day and was continued weekly thereafter. Therapeutic infusions of AURKA$_{207-215}$–specific *TCR* gene-modified CD8$^+$ T cells significantly suppressed tumor growth ($P < .02$). Error bars represent SDs.

Although adoptive antileukemia/lymphoma therapy with redirected T cells using tumor antigen-specific *TCR* or *CAR* gene transfer remains in its infancy, emerging evidence supports the development of such therapeutic options.

A number of preclinical and clinical studies of tumor antigen-specific *TCR* gene therapy have underscored the fact that appropriate antigen selection is essential to minimize the likelihood of on-target adverse events mediated by redirected T cell recognition of normal tissues expressing self-derived specificities.[39] This concept is further supported by a recent study of NY-ESO-1–specific *TCR* gene transfer.[19] In this report, objective clinical responses were observed in 5 of 11 patients with metastatic melanoma and 4 of 6 patients with metastatic synovial cell sarcoma without any toxicity related to engineered T cell activity.[19] Thus, the exploration of novel tumor antigens to identify safe and effective targets for *TCR* gene therapy is warranted, especially in the context of hematologic malignancies.

Previously, we reported a significant correlation between the overexpression of *AURKA* mRNA and the aggressiveness of lymphoma cells.[13] Furthermore, we found that *AURKA* mRNA is overexpressed in a large proportion of freshly isolated human leukemia cells.[6] However, in normal tissues, *AURKA* mRNA expression is largely limited to the testis.[13] Subsequently, we identified an immunogenic nonamer epitope derived from AURKA that was presented in the context of HLA-A*0201.[6] In the present study, we set out to examine the feasibility of redirected T cell–based adoptive immunotherapy for the treatment of human leukemia using a TCR derived from an HLA-A*0201–restricted AURKA$_{207-215}$–specific CD8$^+$ T-cell clone (AUR-2). Expression of this TCR in CD8$^+$ T cells conferred antileukemia reactivity both in vitro and in a xenogeneic mouse model of human leukemias. Furthermore, CD4$^+$ T cells could be redirected using this TCR to recognize the same HLA-A*0201–restricted AURKA$_{207-215}$ epitope. This represents a potentially important advantage, as the same TCR could redirect both helper (CD4$^+$) and cytotoxic (CD8$^+$) functions within the transduced T-cell population, which might sustain the antileukemia response in vivo after adoptive transfer.

Redirected CD8$^+$ T cells expressing the *TCR* cloned from AUR-2 displayed similar levels of functional sensitivity to the parental CTL clone. In vitro, AURKA$_{207-215}$–specific *TCR* gene-transduced CD8$^+$ T cells were able to lyse HLA-A*0201$^+$ human leukemia line GANMO-1 cells, which overexpress *AURKA* mRNA, and freshly isolated leukemia cells from HLA-A*0201$^+$ patients. This antileukemia reactivity was implemented through recognition of the endogenously processed AURKA$_{207-215}$ epitope presented in the context of HLA-A*0201. Importantly, these AURKA$_{207-215}$-specific *TCR*-transduced CD8$^+$ T cells did not lyse HLA-A*0201$^+$ normal PBMCs, mitotic PHA-lymphoblasts or cord blood CD34$^+$ cells; these data suggest that on-target adverse effects would be minimal in clinical applications. Furthermore, we demonstrated the efficacy of AURKA$_{207-215}$–specific *TCR*-transduced CD8$^+$ T cells in vivo by showing the inhibition of leukemia cell growth in a xenograft mouse model. As many hematopoietic progenitor cells actively proliferate and will therefore have enhanced AURKA expression levels, these cells may become targets for AURKA$_{207-215}$–specific *TCR*-transduced CD8$^+$ T cells in vivo, as is the case with selective AURKA inhibitors.[40] However, our observations suggest that redirected CD8$^+$ T cells targeting AURKA may not cause severe bone marrow failure, although further studies are needed to substantiate this point.

Notably, AURKA is overexpressed in the fraction of bone marrow cells that encompasses myeloid leukemia stem cells.[6,41] Recently, targeting leukemia stem cells has been highlighted as a treatment strategy to prevent disease progression in a durable fashion.[42] Monoclonal antibodies that target leukemia stem cell surface antigens have been proposed for this purpose. Examples of such molecules include CD123 (IL3Rα)[43] and TIM-3.[44] Cellular immunotherapy targeting antigens that are preferentially overexpressed in leukemia stem cells has also been proposed. In this regard, WT1 appears to be a particularly attractive candidate.[45] Indeed, we have cloned an HLA-A*2402–restricted WT1$_{235-243}$–specific *TCR* gene into our unique si-*TCR* vector to address the potential of this approach.[46] With respect to AURKA, we previously described that the CD34$^+$CD38$^-$ fraction of bone marrow mononuclear cells from CML patients expressed high levels of *AURKA* mRNA and that these cells were susceptible to AURKA-specific CTL-mediated lysis.[6] Thus, redirected T cell–based immunotherapy targeting AURKA might be able to suppress leukemia stem cells. Furthermore, such an approach may be synergistic with the administration of selective AURKA inhibitors, for example in the treatment of relapsed leukemia after allogeneic hematopoietic stem cell transplantation.

Strategic options to achieve better clinical responses in the field of *TCR* gene transfer are much needed. The manipulation of helper CD4$^+$ T cells is one such approach.[24,47,48] To date, the adoptive transfer of redirected CD4$^+$ T cells concurrently with CD8$^+$ T cells expressing the same tumor-specific TCR gene has not been described; however, this is an intriguing notion that could enhance the antitumor reactivity of such adoptive transfer approaches in vivo. In recognition of this possibility, we found that AURKA$_{207-215}$ *TCR*-transduced CD4$^+$ T cells displayed Th1 cytokine production in response to the HLA-A*0201/AURKA$_{207-215}$ epitope in vitro. The effects of such activity in vivo, however, remain to be clarified. Another approach to combined immunotherapy employs peptide vaccination. Indeed, vaccination with the relevant peptide has been

shown to enhance the antitumor functionality of infused gene-modified T cells.[49] The feasibility of this combination strategy using $AURKA_{207-215}$ peptide vaccination is currently under investigation.

In summary, we have demonstrated the feasibility of antileukemia adoptive therapy using AURKA-specific *TCR* gene transfer. As AURKA is also overexpressed in diverse solid tumors,[4] the potential clinical applications of this approach are widespread. Further studies are therefore warranted to investigate the safety and utility of this novel therapy in the clinic.

Acknowledgments

The authors are grateful for the skilled technical assistance of Dr Kenji Kameda, Ehime University, Japan. They also thank Dr Midori Okumura and Dr Tomihiro Katayama, Department of Obstetrics and Gynecology, Ehime University Graduate School of Medicine, Japan, for supplying cord blood samples; Dr Hiroo Saji, HLA Laboratory, Japan, for HLA typing, Dr Erik Hooijberg; Vrije Universiteit Medisch Centrum, The Netherlands, for supplying the Jurkat/MA cell line; and Dr A. John Barrett, National Heart, Lung, and Blood Institute, National Institutes of Health, for supplying the C1R-A2 cell line.

This work was supported in part by grants from the Ministry of Education, Culture, Sports, Science and Technology of Japan to T.O., H.F., and M.Y., a Grant-in-Aid for Cancer Research from the Ministry of Health, Labor and Welfare to M.Y., and a grant from the Third Term Comprehensive Control Research for Cancer to K.K. D.A.P. is a Medical Research Council (United Kingdom) Senior Clinical Fellow.

Authorship

Contribution: K.N. and T.O. performed the research and wrote the paper; H.F. designed and performed the research, wrote and edited the paper, and provided financial support; J.A., T.S., J.M., H.S., J.J.M., and E.I. discussed and interpreted the experimental results and provided materials; K.K., E.G., and D.A.P. made and supplied the tetramers and edited the paper; and M.Y. discussed and interpreted the experimental results, edited the paper, and provided financial support.

Conflict-of-interest disclosure: The authors declare no competing financial interests.

Correspondence: Hiroshi Fujiwara, Department of Bioregulatory Medicine, Ehime University Graduate School of Medicine, Toon, Ehime 791-0295, Japan; e-mail: yunarief@m.ehime-u.ac.jp; or Masaki Yasukawa, Department of Bioregulatory Medicine, Ehime University Graduate School of Medicine, Toon, Ehime 791-0295, Japan; e-mail: yasukawa@m.ehime-u.ac.jp.

References

1. Marumoto T, Zhang D, Saya H. Aurora-A-a guardian of poles. *Nat Rev Cancer.* 2005;5(1):42-50.
2. Carmena M, Earnshaw WC. The cellular geography of aurora kinases. *Nat Rev Mol Cell Biol.* 2003;4(11):842-845.
3. Bischoff JR, Anderson L, Zhu Y, et al. A homologue of Drosophila aurora kinase is oncogenic and amplified in human colorectal cancers. *EMBO J.* 1998;17(11):3052-3065.
4. Gautschi O, Heighway J, Mack PC, Pumell PR, Lara PN Jr, Gandara DR. Aurora kinases as an anticancer targets. *Clin Cancer Res.* 2008;14(6):1639-1648.
5. Ikezoe T, Yang J, Nishioka C, et al. A novel treatment strategy targeting Aurora kinases in acute myelogenous leukemia. *Mol Cancer Ther.* 2007;6(6):1851-1857.
6. Ochi T, Fujiwara H, Suemori K, et al. Aurora-A kinase: a novel target of cellular immunotherapy for leukemia. *Blood.* 2009;113(1):66-74.
7. Ewart-Toland A, Briassouli P, de Koning JP, et al. Identification of Stk6/STK15 as a candidate low-penetrance tumor-susceptibility gene in mouse and human. *Nat Genet.* 2003;34(4):403-412.
8. Xu HT, Ma L, Qi FJ, et al. Expression of serine threonine kinase 15 is associated with poor differentiation in lung squamous cell carcinoma and adenocarcinoma. *Pathol Int.* 2006;56(7):375-380.
9. Boss DS, Beijnen JH, Schellens JH. Clinical experience with aurora kinase inhibitors: a review. *Oncologist.* 2009;14(8):780-793.
10. Dees EC, Infante JR, Cohen RB, et al. Phase 1 study of MLN8054, a selective inhibitor of Aurora A kinase in patients with advanced solid tumors. *Cancer Chemother Pharmacol.* 2011;67(4):945-954.
11. Steeghs N, Eskens FA, Gelderblom H, et al. Phase I pharmacokinetic and pharmacodynamic study of the aurora kinase inhibitor danusertib in patients with advanced or metastatic solid tumors. *J Clin Oncol.* 2009;27(30):5094-5101.
12. Traynor AM, Hewitt M, Liu G, et al. Phase I dose escalation study of MK-0457, a novel Aurora kinase inhibitor, in adult patients with advanced solid tumors. *Cancer Chemother Pharmacol.* 2011;67(2):305-314.
13. Hamada M, Yakushijin Y, Ohtsuka M, Kakimoto M, Yasukawa M, Fujita S. Aurora2/BTAK/STK15 is involved in cell cycle checkpoint and cell survival of aggressive non-Hodgkin's lymphoma. *Br J Haematol.* 2003;121(3):439-447.
14. Kobayashi H, Azumi M, Hayashi S, et al. Characterization of human CD4 helper T cell responses against Aurora kinase A. *Cancer Immunol Immunother.* 2010;59(7):1029-1039.
15. Morgan RA, Dudley ME, Wunderlich JR, et al. Cancer regression in patients after transfer of genetically engineered lymphocytes. *Science.* 2006;314(5796):126-129.
16. Johnson LA, Morgan RA, Dudley ME, et al. Gene therapy with human and mouse T-cell receptors mediates cancer regression and targets normal tissues expressing cognate antigen. *Blood.* 2009;114(3):535-546.
17. Bendle GM, Linnemann C, Hooijkaas AI, et al. Lethal graft-versus-host disease in mouse models of T cell receptor gene therapy. *Nat Med.* 2010;16(5):565-570.
18. Okamoto S, Mineno J, Ikeda H, et al. Improved expression and reactivity of transduced tumor-specific TCRs in human lymphocytes by specific silencing of endogenous TCR. *Cancer Res.* 2009;69(23):9003-9011.
19. Robbins PF, Morgan RA, Feldman SA, et al. Tumor regression in patients with metastatic synovial cell sarcoma and melanoma using genetically engineered lymphocytes reactive with NY-ESO-1. *J Clin Oncol.* 2011;29(7):917-924.
20. Calogero A, Hospers GA, Krüse KM, et al. Retargeting of a T cell line by anti MAGE-3/HLA-A2 alpha beta TCR gene transfer. *Anticancer Res.* 2000;20(3A):1793-1799.
21. Price DA, Brenchly JM, Ruff LE, et al. Avidity for antigen shapes clonal dominance in CD8+ T cell populations specific for persistent DNA viruses. *J Exp Med.* 2005;202(10):1349-1361.
22. Kuzushima K, Hayashi N, Kimura H, Tsurumi T. Efficient identification of HLA-A*2402-restricted cytomegalovirus-specific $CD8^+$ T-cell epitopes by a computer algorithm and an enzyme-linked immunospot assay. *Blood.* 2001;98(6):1872-1881.
23. Ohminami H, Yasukawa M, Fujita S. HLA class I-restricted lysis of leukemia cells by a $CD8^+$ cytotoxic T-lymphocyte clone specific for WT1 peptide. *Blood.* 2000;95(1):286-293.
24. Tsuji T, Yasukawa M, Matsuzaki J, et al. Generation of tumor-specific, HLA class I-restricted human Th1 and Tc1 cells by cell engineering with tumor peptide-specific T-cell receptor genes. *Blood.* 2005;106(2):470-476.
25. Folch G, Scaviner D, Contet V, Lefranc MP. Protein displays of the human T cell receptor alpha, beta, gamma and delta variable and joining regions. *Exp Clin Immunogenet.* 2000;17(4):205-215.
26. Arden B, Clark SP, Kabelitz D, Mak TW. Human T-cell receptor variable gene segment families. *Immunogenetics.* 1995;42(6):455-500.
27. Jedema I, van der Werff NM, Barge RM, Willemze R, Falkenburg JH. New CFSE-based assay to determine susceptibility to lysis by cytotoxic T cells of leukemic precursor cells within a heterogeneous target cell population. *Blood.* 2004;103(7):2677-2682.
28. Yasukawa M, Ohminami H, Arai J, Kasahara Y, Ishida Y, Fujita S. Granule exocytosis, and not the fas/fas ligand system, is the main pathway of cytotoxicity mediated by alloantigen-specific $CD4^+$ as well as $CD8^+$ cytotoxic T lymphocytes in humans. *Blood.* 2000;95(7):2352-2355.
29. Ito M, Hiramatsu H, Kobayashi K, et al. NOD/SCID/gamma(c) (null) mouse: an excellent recipient mouse model for engraftment of human cells. *Blood.* 2002;100(9):3175-3182.
30. Xue SA, Gao L, Hart D, at al. Elimination of human leukemia cells in NOD/SCID mice by WT1-TCR gene-transduced human T cells. *Blood.* 2005;106(9):3062-3067.
31. Finney HM, Akbar AN, Lawson AD. Activation of

resting human primary T cells with chimeric receptors: costimulation from CD28, inducible costimulator, CD134, and CD137 in series with signals from the TCR zeta chain. *J Immunol.* 2004; 172(1):104-113.

32. Brentjens RJ, Santos E, Nikhamin Y, et al. Genetically targeted T cells eradicate systemic acute lymphoblastic leukemia xenografts. *Clin Cancer Res.* 2007;13(18 Pt 1):5426-5435.
33. Hollyman D, Stefanski J, Przybylowski M, et al. Manufacturing validation of biologically functional T cells targeted to CD19 antigen for autologous adoptive cell therapy. *J Immunother.* 2009;32(2): 169-180.
34. Wang J, Press OW, Lindgren CG, et al. Cellular immunotherapy for follicular lymphoma using genetically modified CD20-specific $CD8^+$ cytotoxic T lymphocytes. *Mol Ther.* 2004;9(4):577-586.
35. James SE, Greenberg PD, Jensen MC, et al. Antigen sensitivity of CD22-specific chimeric TCR is modulated by target epitope distance from the cell membrane. *J Immunol.* 2008;180(10):7028-7038.
36. Hombach A, Muche JM, Gerken M, et al. T cells engrafted with a recombinant anti-CD30 receptor target autologous $CD30^+$ cutaneous lymphoma cells. *Gene Ther.* 2001;8(11):891-895.
37. Hudecek M, Schmitt TM, Baskar S, et al. The B-cell tumor-associated antigen ROR1 can be targeted with T cells modified to express a ROR1-specific chimeric antigen receptor. *Blood.* 2010; 116(22):4532-4541.
38. Till BG, Jensen MC, Wang J, et al. Adoptive immunotherapy for indolent non-Hodgkin lymphoma and mantle cell lymphoma using genetically modified autologous CD20-specific T cells. *Blood.* 2008;112(6):2261-2271.
39. Offringa R. Antigen choice in adoptive T-cell therapy of cancer. *Curr Opin Immunol.* 2009; 21(2):190-199.
40. Moore AS, Blagg J, Linardopoulos S, Pearson ADJ. Aurora kinase inhibitors: novel small molecules with promising activity in acute and Philadelphia-positive leukemias. *Leukemia.* 2010;24: 671-678.
41. Ye D, Garcia-Manero G, Kantarjian HM, et al. Analysis of Aurora kinase A expression in $CD34^+$ blast cells isolated from patients with myelodysplastic syndromes and acute myeloid leukemia. *J Hematop.* 2009;2(1):2-8.
42. Misaghian N, Ligresti G, Steelman LS, et al. Targeting the leukemic stem cell: the Holy Grail of leukemia therapy. *Leukemia.* 2009;23(1):25-42.
43. Jin L, Lee EM, Ramshaw HS, et al. Monoclonal antibody-mediated targeting of CD123, IL-3 receptor alpha chain, eliminates human acute myeloid leukemic stem cells. *Cell Stem Cell.* 2009; 5(1):31-42.
44. Kikushige Y, Shima T, Takayanagi S, et al. TIM-3 is a promising target to selectively kill acute myeloid leukemia stem cells. *Cell Stem Cell.* 2010; 7(6):708-717.
45. Saito Y, Kitamura H, Hijikata A, et al. Identification of therapeutic targets for quiescent, chemotherapy-resistant human leukemia stem cells. *Sci Transl Med.* 2010;2(17):17ra9.
46. Ochi T, Fujiwara H, Okamoto S, et al. Novel adoptive T-cell immunotherapy using a WT1-specific TCR vector encoding silencers for endogenous TCRs show marked antileukemia reactivity and safety. *Blood.* 2011;118(6):1495-1503.
47. Morris EC, Tsallios A, Bendle GM, Xue SA, Stauss HJ. A critical role of T cell antigen receptor-transduced MHC class I-restricted helper T cells in tumor protection. *Proc Natl Acad Sci U S A.* 2005;102(22):7934-7939.
48. Ray S, Chhabra A, Chakraborty NG, et al. MHC-I-restricted melanoma antigen specific TCR-engineered human $CD4^+$ T cells exhibit multifunctional effector and helper responses, in vitro. *Clin Immunol.* 2010;136(3):338-347.
49. Ly LV, Sluijter M, Versluis M, et al. Peptide vaccination after T-cell transfer causes massive clonal expansion, tumor eradication, and manageable cytokine storm. *Cancer Res.* 2010;70(21):8339-8346.

Rapid diagnosis of FHL3 by flow cytometric detection of intraplatelet Munc13-4 protein

Yuuki Murata,[1] Takahiro Yasumi,[1] Ryutaro Shirakawa,[2] Kazushi Izawa,[1] Hidemasa Sakai,[1] Junya Abe,[1] Naoko Tanaka,[1] Tomoki Kawai,[1] Koichi Oshima,[3-5] Megumu Saito,[3] Ryuta Nishikomori,[1] Osamu Ohara,[4,5] Eiichi Ishii,[6] Tatsutoshi Nakahata,[3] Hisanori Horiuchi,[2] and Toshio Heike[1]

[1]Department of Pediatrics, Kyoto University Graduate School of Medicine, Kyoto, Japan; [2]Department of Molecular and Cellular Biology, Institute of Development, Aging and Cancer, Tohoku University, Sendai, Japan; [3]Clinical Application Department, Center for iPS Cell Research and Application, Kyoto University, Kyoto, Japan; [4]Department of Human Genome Research, KAZUSA DNA Research Institute, Kisarazu, Japan; [5]Laboratory for Immunogenomics, Research Center for Allergy and Immunology, RIKEN, Yokohama, Japan; and [6]Department of Pediatrics, Ehime University Graduate School of Medicine, Toon, Japan

Familial hemophagocytic lymphohistiocytosis (FHL) is a potentially lethal genetic disorder of immune dysregulation that requires prompt and accurate diagnosis to initiate life-saving immunosuppressive therapy and to prepare for hematopoietic stem cell transplantation. In the present study, 85 patients with hemophagocytic lymphohistiocytosis were screened for FHL3 by Western blotting using platelets and by natural killer cell lysosomal exocytosis assay. Six of these patients were diagnosed with FHL3. In the acute disease phase requiring platelet transfusion, it was difficult to diagnose FHL3 by Western blot analysis or by lysosomal exocytosis assay. In contrast, the newly established flow cytometric analysis of intraplatelet Munc13-4 protein expression revealed bimodal populations of normal and Munc13-4–deficient platelets. These findings indicate that flow cytometric detection of intraplatelet Munc13-4 protein is a sensitive and reliable method to rapidly screen for FHL3 with a very small amount of whole blood, even in the acute phase of the disease. (*Blood.* 2011;118(5):1225-1230)

Introduction

The granule-dependent cytotoxic pathway is a major immune effector mechanism used by cytotoxic T lymphocytes (CTLs) and natural killer (NK) cells.[1] The pathway involves a series of steps, including cell activation, polarization of the lysosomal granules to the immunologic synapse, exocytosis of lytic proteins such as perforin and granzymes, and induction of apoptosis in the target cells.[2] In addition to its central role in the defense against intracellular infections and in tumor immunity, this pathway also plays an important role in the regulation of immune homeostasis. Defects in the granule-dependent cytotoxic pathway result in a catastrophic hyperinflammatory condition known as hemophagocytic lymphohistiocytosis (HLH).[1,3]

HLH is a life-threatening syndrome of immune dysregulation resulting from the uncontrolled activation and proliferation of CTLs, which leads to macrophage activation and the excessive release of inflammatory cytokines.[4,5] Clinical diagnosis of HLH is made on the basis of cardinal signs and symptoms including prolonged fever and hepatosplenomegaly, and by characteristic laboratory findings such as pancytopenia, hyperferritinemia, hypofibrinogenemia, increased levels of soluble IL-2 receptor, and low or absent NK cell activity.[5,6] HLH can be classified into primary (genetic) or secondary (acquired) forms according to the underlying etiology, although this distinction is difficult to make in clinical practice.[4,5]

Familial hemophagocytic lymphohistiocytosis (FHL) encompasses major forms of primary HLH for which mutations in the genes encoding perforin (*PRF1*; FHL2),[7] Munc13-4 (*UNC13D*; FHL3),[8] syntaxin-11 (*STX11*; FHL4),[9] and syntaxin-binding protein 2 (also known as Munc18-2) (*STXBP2*; FHL5)[10,11] have been identified to date. Perforin is a cytolytic effector that forms a pore-like structure in the target cell membrane. Munc13-4, syntaxin-11, and Munc18-2 are involved in intracellular trafficking or the fusion of cytolytic granules to the plasma membrane and the subsequent delivery of their contents into target cells.[1,12] Consequently, defective cytotoxic activity of CTLs and NK cells is one of the hallmark findings of FHL,[7,8,13-16] although NK cell activity is also decreased in some cases of secondary HLH.[15,17-20]

Prompt and accurate diagnosis of FHL is mandatory to initiate life-saving immunosuppressive therapy and to prepare for hematopoietic stem cell transplantation. Detection of perforin expression in NK cells with flow cytometry is a reliable method to screen for FHL2.[21] Another test analyzes the expression of CD107a on the surface of NK cells, which marks the release of cytolytic granules.[22] Reduced expression of CD107a implies impaired degranulation of NK cells and predicts a likelihood of FHL3.[23] However, this analysis is not available in some patients with extremely reduced NK cell numbers, such as during the acute phase of HLH.[19] In addition, NK-cell degranulation is also impaired in FHL4[24] and FHL5,[10,11] making it impossible to differentiate these disorders.

We reported previously that Munc13-4 protein is expressed in platelets and regulates the secretion of dense core granules.[25] Herein we report that Munc13-4 is expressed far more abundantly in platelets than in PBMCs. We also describe the development of a

Submitted January 10, 2011; accepted May 23, 2011. Prepublished online as *Blood* First Edition paper, June 8, 2011; DOI 10.1182/blood-2011-01-329540.

The online version of this article contains a data supplement.

The publication costs of this article were defrayed in part by page charge payment. Therefore, and solely to indicate this fact, this article is hereby marked "advertisement" in accordance with 18 USC section 1734.

new method to screen for FHL3 rapidly by detecting intraplatelet Munc13-4 expression through flow cytometry.

Methods

Patients

Between January 2008 and March 2010, whole blood samples from 85 patients were screened for FHL3. The patients had been clinically diagnosed with HLH by their referring physicians and were suspected of possible FHL. Characteristics of the enrolled patients are summarized in supplemental Table 1 (available on the *Blood* Web site; see the Supplemental Materials link at the top of the online article). As a control, blood obtained from healthy adults at the time of patient sampling was shipped for screening along with the patient samples. Before the laboratory studies were performed, informed consent was obtained from the patients and their parents, in accordance with the institutional review board of Kyoto University Hospital and the Declaration of Helsinki.

Preparation of PBMCs and platelet samples

Whole blood samples treated with EDTA were centrifuged gently at 100*g* for 10 minutes, and platelets were collected from the supernatant plasma layer. Alternatively, platelets were prepared from small aliquots of blood samples by lysing red blood cells with ammonium chloride. PBMCs were obtained by Ficoll-Hypaque density gradient centrifugation from the remaining sample. $CD4^+$, $CD8^+$, $CD14^+$, $CD19^+$, and $CD45^+$ cells were separated from PBMCs using an AutoMACS Pro (Miltenyi Biotec) and magnetic bead–conjugated mAbs according to the manufacturer's instructions. Flow cytometric analysis revealed that each cell population contained > 95% $CD4^+$, $CD8^+$, $CD14^+$, $CD19^+$, and $CD45^+$ cells (data not shown).

Mutation analysis

Genomic DNA was isolated from the PBMCs of patients with defective Munc13-4 expression using standard procedures. Primers were designed for the amplification and direct DNA sequencing of the *UNC13D*-coding exons, including the adjacent intronic sequences for the identification of splice-site variants. Primer sequences are available upon request. Products were sequenced directly with an ABI3130 genetic analyzer (Applied Biosystems).

Antibodies

Rabbit polyclonal antibodies raised against the N-terminal region (residues 1-262)[25] and full-length human Munc13-4 protein were used as primary antibodies for Western blot and flow cytometric analysis, respectively. Rabbit polyclonal anti-integrin αIIb (Santa Cruz Biotechnology) and mouse polyclonal anti–β-actin (Sigma-Aldrich) antibodies were used as primary antibodies for Western blotting. The mAbs used in the flow cytometric analysis were FITC-conjugated anti-CD3 (SK7; BD Pharmingen), phycoerythrin (PE)–conjugated anti-CD41a (HIP8; BD Pharmingen); allophycocyanin-conjugated anti-CD56 (N901; Beckman Coulter), and PE-conjugated anti-CD107a (H4A3; eBioscience).

Western blot analysis

Cell extracts were fractionated by SDS-PAGE, and the fractionated proteins were electrotransferred onto polyvinylidene fluoride membranes. The membranes were blocked overnight in blocking buffer (5% skim milk) and incubated for 1 hour at room temperature with the primary antibodies, followed by HRP-conjugated anti–rabbit or anti–mouse IgG polyclonal antibodies (Santa Cruz Biotechnology). Specific bands were visualized by the standard enhanced chemiluminescence method.

Flow cytometric analysis of Munc13-4 protein

After surface staining with anti-CD41a mAbs, platelets were fixed and permeabilized by Cytofix/Cytoperm (BD Biosciences) and washed 3 times with Perm/Wash buffer (BD Biosciences). After nonspecific reactions were blocked with Chrome-Pure human IgG (Jackson ImmunoResearch Laboratories), rabbit polyclonal antibody against the full-length human Munc13-4 protein was added, followed by FITC-conjugated donkey anti–rabbit IgG (Jackson ImmunoResearch Laboratories). Platelets were gated on the basis of their appearance on forward- and side-scatter plots in log/log scale and by CD41a expression. The gated platelets were analyzed for Munc13-4 expression by flow cytometry (FACSCalibur; BD Biosciences).

Lysosomal degranulation assays

To quantify lysosome exocytosis by NK cells, 2×10^5 PBMCs were mixed with 2×10^5 human erythroleukemia cell line K562 cells and incubated for 2 hours in complete medium (RPMI 1640 medium supplemented with 2mM L-glutamine and 10% FCS) at 37°C in 5% CO_2. Cells were resuspended in PBS supplemented with 2% FCS and 2mM EDTA; stained with anti-CD3–FITC, anti-CD56–allophycocyanin, and anti-CD107a–PE mAbs; and analyzed by flow cytometry.

Platelet exocytosis of the lysosomal granules was analyzed as described previously[26] but with a minor modification. Briefly, platelets were suspended in PBS containing 2mM EDTA and PE-conjugated anti-CD107a mAb, stimulated with 5 U/mL of thrombin (Wako Pure Chemical Industries) for 10 minutes at 25°C, and immediately analyzed by flow cytometry. The degranulation index of platelets was calculated as: (mean fluorescence value of stimulated sample − mean fluorescence value of nonstimulated sample)/mean fluorescence value of nonstimulated sample.

Statistical analysis

Statistical analyses were performed with 1-way ANOVA followed by the Tukey post hoc test to compare multiple groups, with a $P < .05$ level considered to be significant.

Results

Diagnosis of FHL3 by Western blot analysis using platelets

Before screening for FHL3, the Munc13-4 expression level was compared between platelets and PBMCs. Munc13-4 expression in platelets was approximately 10 times higher than that in PBMCs (Figure 1A). $CD8^+$ cells expressed a similar level of Munc13-4 protein as other PBMC cell types (Figure 1B). Similar amounts of platelet- and PBMC-derived proteins could be obtained from a sample (data not shown). Therefore, platelets were used to perform Western blotting to screen for Munc13-4 deficiency. Of the 85 patients screened, 6 patients were diagnosed with FHL3 (Figure 1C). Munc13-4 protein was barely detected in the platelets of each FHL3 patient regardless of the gene mutation (Table 1). For each sample, no more than 1 mL of whole blood was required to perform the analysis.

Difficulty in diagnosing FHL3 in the acute phase of the disease

Patients in the acute phase of the disease who require screening for FHL often receive platelet transfusions because of thrombocytopenia.[4-6] To study the effect of transfused platelets on screening results, FHL3 screening was attempted in a patient receiving platelet transfusions. As expected, Western blotting using platelets could not detect Munc13-4 deficiency because of the normal expression of the protein in the transfused platelets (Figure 2A left column). Surprisingly, Western blotting using PBMCs also could not clearly identify Munc13-4 deficiency because a substantial number of platelets were present in the PBMCs obtained by the standard method (Figure 2A right column). By positively selecting $CD45^+$ cells and removing platelets, it was found that a considerable amount of the Munc13-4 protein detected in PBMC samples

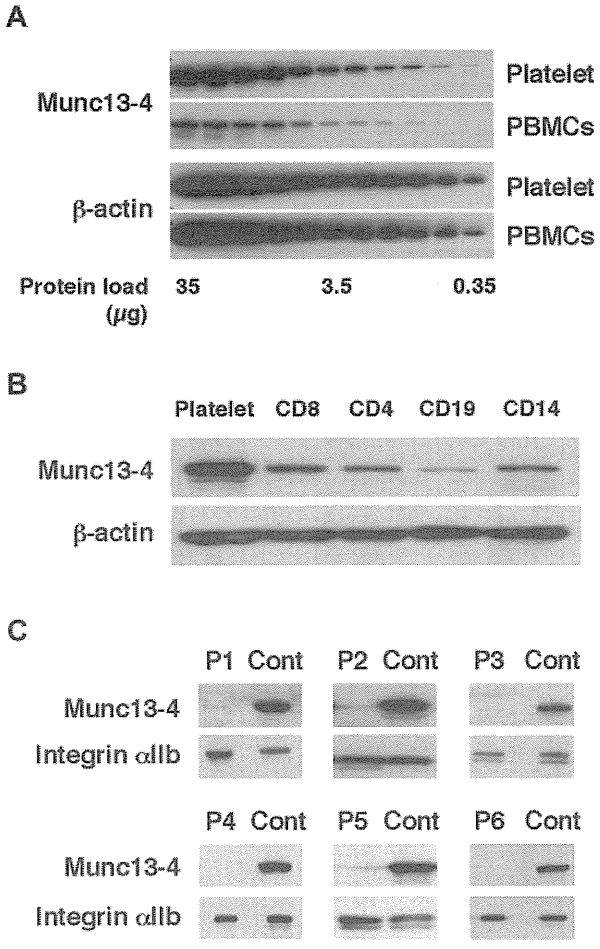

Figure 1. Diagnosing FHL3 by Western blotting using platelet protein. The amount of Munc13-4 protein expression was compared between platelets and PBMCs (A) and among platelets, $CD8^+$, $CD4^+$, $CD19^+$, and $CD14^+$ cells (B) by Western blotting. A representative result of 5 independent experiments is shown. (C) Six FHL3 patients were diagnosed by Western blotting for Munc13-4 protein using platelets.

obtained by standard density gradient centrifugation was actually derived from the contaminating platelets (Figure 2B).

We performed a NK-cell degranulation assay for every referred sample and found the assay to be defective for every FHL3 patient identified (data not shown). All of the other patients showed a normal release of lysosomal granules by NK cells; however, the analysis could not be performed in some patients because of the extremely low NK-cell number during the acute phase of the disease (data not shown).

We also examined the lysosomal granule release of platelets in 31 patients to determine whether this assay could be used as a screening method for FHL3. Lysosomal exocytosis of FHL3 platelets was partially impaired at steady state, but profound impairment was observed during the acute phase of the disease (Figure 3A-C). This profound impairment was also observed in platelets obtained from some secondary HLH patients during the acute phase (Figure 3B-C). These results indicate that it is difficult to diagnose FHL3 during the acute phase of HLH either by Western blot or by lysosomal degranulation assay.

Table 1. UNC13D gene mutations of FHL3 patients

Patient	Age at onset	Gender	Mutation	Genotype	Predicted effect
P1	14 days	Female	c.1596 + 1G → C	Homo	Splice error
P2	2 months	Male	c.322–1G → A	Hetero	Splice error
			c.990G → C	Hetero	p.Q330H
			c.3193C → T	Hetero	p.R1065X
P3	12 months	Female	c.754–1G → C	Hetero	Splice error
			c.2485delC	Hetero	p.L829fs
P4	4 months	Female	c.754–1G → C	Hetero	Splice error
			c.1799C → T	Hetero	p.T600M
			c.1803C → A	Hetero	p.Y601X
P5	2 months	Female	c.754–1G → C	Hetero	Splice error
			c.1596 + 1G → C	Hetero	Splice error
P6	5 months	Male	ND	ND	ND

Mutations were checked for single nucleotide polymorphisms using the dbSNP Build 132 database from the National Center for Biotechnology Information.

X indicates stop; fs, frame shift; and ND, not determined.

Rapid diagnosis of FHL3 by flow cytometric detection of intraplatelet Munc13-4

To overcome the difficulty in diagnosing FHL3 during the acute phase of HLH, antibodies were raised against the full-length human Munc13-4 protein (supplemental Figure 1) and a new method was developed to detect Munc13-4 protein in platelets by flow cytometry. A total of 35 patients, including 4 with FHL3 (P3-P6), were

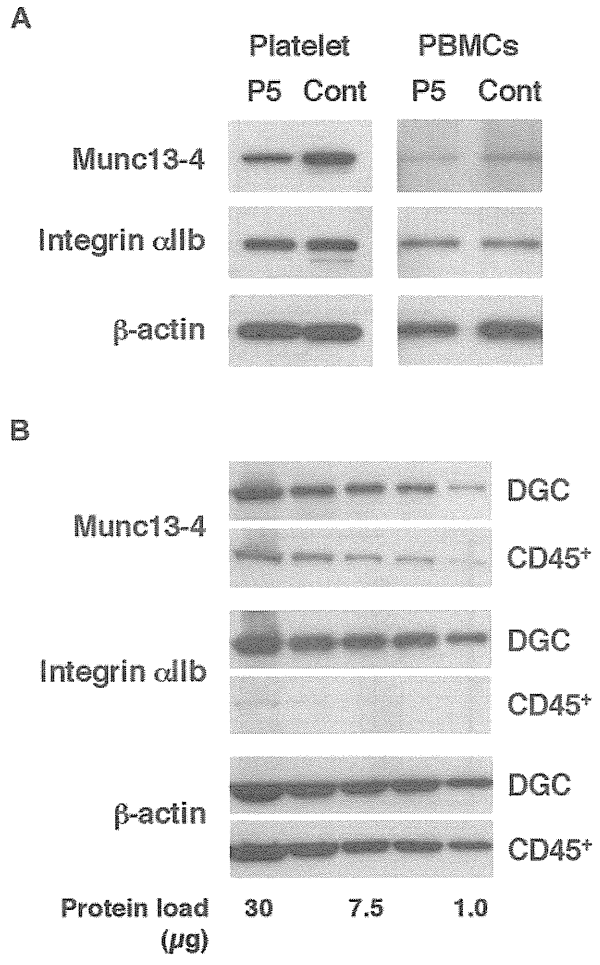

Figure 2. Effect of platelet transfusion on Western blot analysis. (A) Western blotting analysis for Munc13-4 expression using platelets and PBMCs from an FHL3 patient (P5) receiving platelet transfusions during the acute phase of the disease. (B) The expression of Munc13-4 was compared between PBMCs obtained by density gradient centrifugation (DGC) and $CD45^+$ cells obtained by magnetic sorting from healthy controls. A representative result of 3 independent experiments is shown.

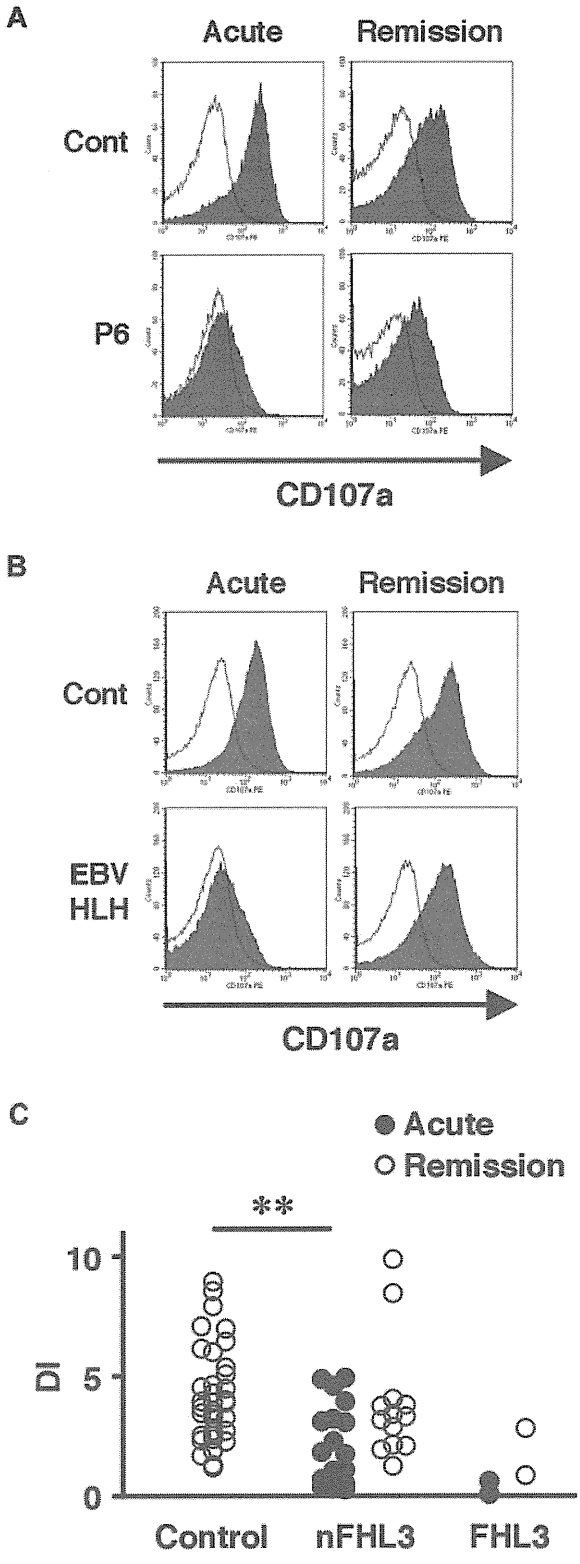

Figure 3. Analysis of lysosomal exocytosis using platelets from HLH patients. Platelets from an FHL3 patient (P6; A) and from a secondary (EBV-associated) HLH patient (B) along with healthy controls were left untreated (open histogram) or were stimulated with thrombin (closed histograms), and the surface expression of CD107a was analyzed by flow cytometry. Analysis was performed during the acute phase of the disease (left column) and after clinical remission (right column). (C) Degranulation index (DI) of platelets from HLH patients during the acute phase (●) and after clinical remission (○). HLH patients with normal NK-cell degranulation and Munc13-4 protein expression by Western blot analysis were defined as non-FHL3 (nFHL3). $^{**}P < .01$ by the Tukey post hoc test.

analyzed using this method. Munc13-4 deficiency was readily detected in all of the FHL3 patients, with a sample volume of < 100 μL of whole blood (Figure 4A-C). Munc13-4 protein was expressed at normal level in the platelets of parents and siblings of FHL3 patients carrying heterozygous *UNC13D* mutations (data not shown). In the FHL3 patient receiving platelet transfusions, flow cytometric analysis revealed bimodal populations of normal and Munc13-4–deficient platelets (P5 in Figure 4A). As shown in Figure 4B, the method was able to clearly identify Munc13-4–deficient platelets in whole blood samples stored at room temperature for 1 week.

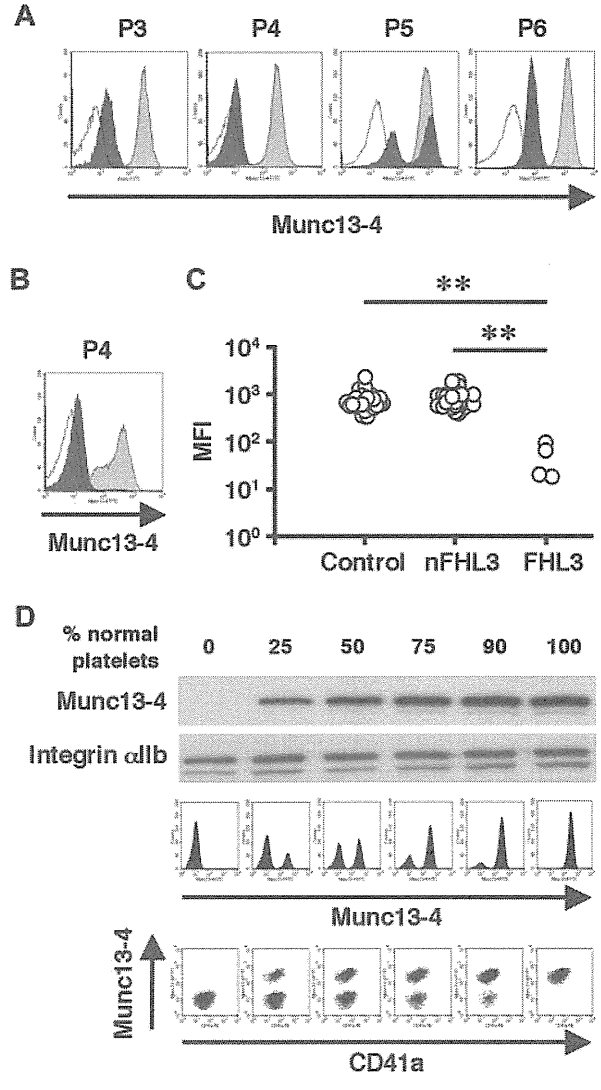

Figure 4. Flow cytometric detection of intraplatelet Munc13-4 protein. Flow cytometric analysis of intraplatelet Munc13-4 expression in 4 FHL3 patients and healthy controls using whole blood samples shipped overnight (A) and in an FHL3 patient (P4) and a healthy control using samples stored at room temperature for a week (B). Dark closed histograms represent platelets from FHL3 patients, whereas light closed histograms represent platelets from healthy controls. Open histograms represent staining with isotype controls. (C) Mean fluorescence intensity (MFI) of intraplatelet Munc13-4 staining for HLH patients and healthy controls. All of the healthy controls (n = 35) were adults. Non-FHL3 (nFHL3) patients (n = 31), as defined in Figure 3, varied in age (2 days-39 years) and included 2 patients with FHL2. Age-related variations in the MFI of Munc13-4 staining were not observed. $^{**}P < .01$ by the Tukey post hoc test. (D) The sensitivities of Western blot and flow cytometric analyses for detecting Munc13-4–deficient platelets were compared.

To determine the sensitivity of the new method, Munc13-4–deficient platelets were mixed with normal platelets at varying ratios. Western blot analysis could not detect Munc13-4–deficient platelets easily, even when the proportion of normal platelets was as low as 25% (Figure 4D). In contrast, flow cytometric analysis easily identified 10% Munc13-4–deficient platelets among 90% normal platelets (Figure 4D), which proved the high sensitivity of the method in diagnosing FHL3.

Discussion

FHL is a rare but life-threatening inherited immune disorder for which mutations in 4 genes have been identified as causative factors. *PRF1* encodes the cytolytic effector protein perforin that forms a pore-like structure in the target cell membrane.[1,12] A mutation in *PRF1* results in FHL2,[7] which accounts for 20%-50% of FHL cases.[4,5] *UNC13D* encodes the protein Munc13-4, which is crucial for the fusion of cytolytic granules to the plasma membrane and the subsequent release of perforin and granzymes.[1,12] Mutations in *UNC13D* result in FHL3,[8] which accounts for 20%-30% of FHL cases.[4,12] FHL4 is caused by mutations in *STX11*, which encodes syntaxin-11.[9] Mutations in *STXBP2*, which encodes Munc18-2, were recently reported to cause FHL5.[10,11] Syntaxin-11 and Munc18-2 also mediate the fusion of cytolytic granules to the plasma membrane.[1,5,12] The ability to screen for FHL2-5 rapidly would facilitate the initiation of life-saving immunosuppressive therapy and the preparation of FHL patients for hematopoietic stem cell transplantation.

In the present study, we found that the Munc13-4 protein is expressed abundantly in platelets (Figure 1A-B). The detection of Munc13-4 protein in platelets by Western blotting (Figure 1C) or flow cytometry (Figure 4A-B) was a reliable screening method to identify FHL3 patients. Munc13-4–deficient platelets were identified easily among normal transfused platelets by flow cytometry, which indicated that this method could be applied to patients who are receiving platelet transfusions during the acute phase of the disease (P5 in Figure 4A). Detection of intraplatelet Munc13-4 was enabled by the use of highly specific antibodies against the full-length human Munc13-4 (supplemental Figure 1).

There is a possibility that FHL3 patients with residual Munc13-4 protein expression could be overlooked by the screening methods described in this study. Most FHL3 patients have mutations that result in the absence or significant reduction of Munc13-4 protein expression,[16,23] as was the case with the patients screened in this study (Figure 1C), which suggests that the mutated Munc13-4 protein is unstable. The NK-cell degranulation assay, which was performed for every referred sample with a sufficient number of NK cells, revealed defective degranulation only in the identified FHL3 patients (date not shown). These results indicate that the majority of mutations in *UNC13D* are likely amenable to rapid detection by the new methods described in this study. Comparative studies on the *UNC13D* genotype, Munc13-4 protein expression, and the lysosomal exocytosis assay must be performed to confirm the reliability of these methods.

It was also investigated whether the analysis of lysosomal release by platelets could be used as an alternative method to screen for FHL3. Profound impairment of lysosomal exocytosis by platelets during the acute phase of the disease and restoration of this impairment after clinical remission was observed in FHL3 and in some secondary HLH patients (Figure 3). It is not clear whether this transient impairment of platelet degranulation is involved in HLH pathogenesis or if it merely reflects in vivo platelet activation by diffuse endothelial damage during the acute phase of the disease that renders them unresponsive to ex vivo stimulation. The release of lysosomal granules by Munc13-4–deficient platelets was impaired only minimally at steady state (Figure 3A and 3C), which is in contrast to a recent study showing the involvement of the Munc13-4 protein in the release of lysosomal granules in mouse platelets.[27] Although the precise reason for this discrepancy is unclear, platelet degranulation is likely to be regulated differentially between species; for example, Munc13-4–deficient mice have bruising and bleeding tendencies[27] that are not commonly associated with human FHL3. Further studies are warranted to elucidate the exocytosis pathways of platelets and their role in the pathophysiology of HLH.

With the development of tools for rapid screening, the diagnostic approach for FHL has changed over the years. Impaired NK cytotoxicity was the first reported signature clinical finding of FHL patients.[13,14] Defective CTL activity was subsequently reported as another hallmark of FHL.[7,8,16,28] However, NK-cell activity is also decreased in some cases of secondary HLH,[15,17-20] and the CTL cytotoxicity assay is not readily accessible to most clinicians. The NK-cell lysosomal exocytosis assay is a comprehensive method to identify patients with a degranulation defect.[10,11,22-24] However, this analysis is not available in some patients with extremely reduced NK-cell numbers, which are often observed during the acute phase of HLH.[19] Although CTLs can be an alternative tool to perform the lysosomal exocytosis assay,[24,28,29] it remains impossible to differentiate FHL3-FHL5.[10,11,23,24] Impairment in these assays warrants the genetic confirmation of FHL, but sequencing all of the candidate genes is not a suitable approach for rapid diagnosis. Flow cytometric detection of perforin expression in NK cells is a reliable and rapid way of identifying patients with FHL2,[21] and the new method described in this study for the detection of Munc13-4 expression in platelets would add to the rapid diagnosis of FHL3.

Platelets could also be used for the screening of FHL4 and FHL5 because they share some granule-transport mechanisms with other types of hematopoietic cells, including CTLs and NK cells.[2,30,31] Indeed, in the present study, both syntaxin-11 and Munc18-2 were expressed abundantly in platelets (data not shown). We are currently using platelet proteins to screen for FHL4-FHL5 by Western blot analysis, although no cases have been found so far because of the extreme rarity of these disorders.

In summary, platelets abundantly express Munc13-4 protein and are a useful tool to screen for FHL3. By detecting intraplatelet Munc13-4 expression by flow cytometry, it is now possible to rapidly screen for FHL3 with a very small sample of whole blood, even in the acute disease phase requiring platelet transfusion. Because platelets share some of their granule transport systems with other types of hematopoietic cells, they could also be used to screen for other types of immune disorders, including FHL4 and FHL5.

Acknowledgments

The authors are grateful to all of the participating patients, their families, and the referring physicians for their generous cooperation in this study.

This study was supported by grants from The Morinaga Foundation for Health and Nutrition; from the Japanese Ministry of

Education, Culture, Sports, Science, and Technology; and from the Japanese Ministry of Health, Labor, and Welfare.

Authorship

Contribution: T.Y., R.N., T.N., H.H., and H.T. designed the research; Y.M., K.I., and M.S. performed the Western blot and flow cytometric analyses; K.O. and O.O. performed the genetic analyses; R.S. and H.H. prepared the anti–Munc13-4 antibodies and started the FHL3 screening; Y.M., T.Y., R.S., K.I., H.S., J.A., N.T., T.K., R.N., E.I., T.N., H.H., and T.H. analyzed and discussed the results; and Y.M., T.Y., and T.H. wrote the manuscript.

Conflict-of-interest disclosure: The authors declare no competing financial interests.

Correspondence: Takahiro Yasumi, Department of Pediatrics, Kyoto University Graduate School of Medicine, 54 Kawahara-cho, Shogoin, Sakyo-ku, Kyoto, 606-8507 Japan; e-mail: yasumi@kuhp.kyoto-u.ac.jp or Hisanori Horiuchi, Department of Molecular and Cellular Biology, Institute of Development, Aging and Cancer, Tohoku University, 4-1 Seiryo-machi, Aoba-ku, Sendai 980-8575 Japan; e-mail: horiuchi@idac.tohoku.ac.jp.

References

1. Fischer A, Latour S, de Saint Basile G. Genetic defects affecting lymphocyte cytotoxicity. *Curr Opin Immunol.* 2007;19(3):348-353.
2. Hong W. Cytotoxic T lymphocyte exocytosis: bring on the SNAREs! *Trends Cell Biol.* 2005; 15(12):644-650.
3. Ménasché G, Feldmann J, Fischer A, de Saint Basile G. Primary hemophagocytic syndromes point to a direct link between lymphocyte cytotoxicity and homeostasis. *Immunol Rev.* 2005;203: 165-179.
4. Janka GE. Familial and acquired hemophagocytic lymphohistiocytosis. *Eur J Pediatr.* 2007; 166(2):95-109.
5. Gupta S, Weitzman S. Primary and secondary hemophagocytic lymphohistiocytosis: clinical features, pathogenesis and therapy. *Expert Rev Clin Immunol.* 2010;6(1):137-154.
6. Créput C, Galicier L, Buyse S, Azoulay E. Understanding organ dysfunction in hemophagocytic lymphohistiocytosis. *Intensive Care Med.* 2008; 34(7):1177-1187.
7. Stepp S, Dufourcq-Lagelouse R, Le Deist F, et al. Perforin gene defects in familial hemophagocytic lymphohistiocytosis. *Science.* 1999;286(5446): 1957-1959.
8. Feldmann J, Callebaut I, Raposo G, et al. Munc13-4 is essential for cytolytic granules fusion and is mutated in a form of familial hemophagocytic lymphohistiocytosis (FHL3). *Cell.* 2003; 115(4):461-473.
9. zur Stadt U, Schmidt S, Kasper B, et al. Linkage of familial hemophagocytic lymphohistiocytosis (FHL) type-4 to chromosome 6q24 and identification of mutations in syntaxin 11. *Hum Mol Genet.* 2005;14(6):827-834.
10. zur Stadt U, Rohr J, Seifert W, et al. Familial hemophagocytic lymphohistiocytosis type 5 (FHL-5) is caused by mutations in Munc18-2 and impaired binding to syntaxin 11. *Am J Hum Genet.* 2009; 85(4):482-492.
11. Côte M, Ménager M, Burgess A, et al. Munc18-2 deficiency causes familial hemophagocytic lymphohistiocytosis type 5 and impairs cytotoxic granule exocytosis in patient NK cells. *J Clin Invest.* 2009;119(12):3765-3773.
12. Cetica V, Pende D, Griffiths GM, Aricò M. Molecular basis of familial hemophagocytic lymphohistiocytosis. *Haematologica.* 2010;95(4):538-541.
13. Perez N, Virelizier JL, Arenzana-Seisdedos F, Fischer A, Griscelli C. Impaired natural killer activity in lymphohistiocytosis syndrome. *J Pediatr.* 1984;104(4):569-573.
14. Aricò M, Nespoli L, Maccario R, et al. Natural cytotoxicity impairment in familial haemophagocytic lymphohistiocytosis. *Arch Dis Child.* 1988;63(3): 292-296.
15. Schneider EM, Lorenz I, Müller-Rosenberger M, Steinbach G, Kron M, Janka-Schaub GE. Hemophagocytic lymphohistiocytosis is associated with deficiencies of cellular cytolysis but normal expression of transcripts relevant to killer-cell-induced apoptosis. *Blood.* 2002;100(8): 2891-2898.
16. Ishii E, Ueda I, Shirakawa R, et al. Genetic subtypes of familial hemophagocytic lymphohistiocytosis: correlations with clinical features and cytotoxic T lymphocyte/natural killer cell functions. *Blood.* 2005;105(9):3442-3448.
17. Schneider EM, Lorenz I, Walther P, Janka-Schaub GE. Natural killer deficiency: a minor or major factor in the manifestation of hemophagocytic lymphohistiocytosis? *J Pediatr Hematol Oncol.* 2003;25(9):680-683.
18. Grom AA, Villanueva J, Lee S, Goldmuntz EA, Passo MH, Filipovich A. Natural killer cell dysfunction in patients with systemic-onset juvenile rheumatoid arthritis and macrophage activation syndrome. *J Pediatr.* 2003;142(3):292-296.
19. Grom AA. Natural killer cell dysfunction: A common pathway in systemic-onset juvenile rheumatoid arthritis, macrophage activation syndrome, and hemophagocytic lymphohistiocytosis? *Arthritis Rheum.* 2004;50(3):689-698.
20. Horne A, Zheng C, Lorenz I, et al. Subtyping of natural killer cell cytotoxicity deficiencies in haemophagocytic lymphohistocytosis provides therapeutic guidance. *Br J Haematol.* 2005;129(5): 658-666.
21. Kogawa K, Lee SM, Villanueva J, Marmer D, Sumegi J, Filipovich AH. Perforin expression in cytotoxic lymphocytes from patients with hemophagocytic lymphohistiocytosis and their family members. *Blood.* 2002;99(1):61-66.
22. Alter G, Malenfant JM, Altfeld M. CD107a as a functional marker for the identification of natural killer cell activity. *J Immunol Methods.* 2004; 294(1-2):15-22.
23. Marcenaro S, Gallo F, Martini S, et al. Analysis of natural killer-cell function in familial hemophagocytic lymphohistiocytosis (FHL): defective CD107a surface expression heralds Munc13-4 defect and discriminates between genetic subtypes of the disease. *Blood.* 2006;108(7): 2316-2323.
24. Bryceson YT, Rudd E, Zheng C, et al. Defective cytotoxic lymphocyte degranulation in syntaxin-11 deficient familial hemophagocytic lymphohistiocytosis 4 (FHL4) patients. *Blood.* 2007;110(6): 1906-1915.
25. Shirakawa R, Higashi T, Tabuchi A, et al. Munc13-4 is a GTP-Rab27-binding protein regulating dense core granule secretion in platelets. *J Biol Chem.* 2004;279(11):10730-10737.
26. Febbraio M, Silverstein RL. Identification and characterization of LAMP-1 as an activation-dependent platelet surface glycoprotein. *J Biol Chem.* 1990;265(30):18531-18537.
27. Ren Q, Wimmer C, Chicka MC, et al. Munc13-4 is a limiting factor in the pathway required for platelet granule release and hemostasis. *Blood.* 2010; 116(6):869-877.
28. Nagai K, Yamamoto K, Fujiwara H, et al. Subtypes of familial hemophagocytic lymphohistiocytosis in Japan based on genetic and functional analyses of cytotoxic T lymphocytes. *PLoS ONE.* 2010;5(11):e14173.
29. Rohr J, Beutel K, Maul-Pavicic A, et al. Atypical familial hemophagocytic lymphohistiocytosis due to mutations in UNC13D and STXBP2 overlaps with primary immunodeficiency diseases. *Haematologica.* 2010;95(12):2080-2087.
30. Stinchcombe J, Bossi G, Griffiths G. Linking albinism and immunity: the secrets of secretory lysosomes. *Science.* 2004;305(5680):55-59.
31. Ren Q, Ye S, Whiteheart SW. The platelet release reaction: just when you thought platelet secretion was simple. *Curr Opin Hematol.* 2008;15(5): 537-541.